CrossMark

Comparing COSMO-CLM simulations and MODIS data of snow cover extent and distribution over Italian Alps

Pierfrancesco Da Ronco[1,2] · **Carlo De Michele**[1] · **Myriam Montesarchio**[2,3] ·
Paola Mercogliano[2,3]

Abstract Snow cover maps from Earth Observation (EO) satellites are valuable datasets containing large-scale information on snow cover extent, snow cover distribution and snow cover duration. In evaluating the performances of Regional Climate Models, EO data can be a valid piece of information alternative to in-situ measurements, which require a dense network of stations covering the entire altitudinal range and techniques for interpolating the values. In this context, MODIS snow products play a leading role providing several types of snow cover maps with high spatial and temporal resolutions. Here, we assess snow cover outputs of a high resolution Regional Climate Model (RCM) using MODIS maps of snow covered area over the Po river basin, northern Italy. The dataset consists of 9 years of MODIS data (2003–2011) cleaned from cloud cover by means of a cloud removal procedure. The maps have 500 m spatial resolution and daily temporal resolution. The RCM considered is COSMO-CLM, run at 0.0715° resolution (about 8 km) and coupled with the soil module TERRA_ML. The ERA-Interim reanalyses are used as initial and boundary conditions. The results show a good agreement between observed and simulated snow cover duration and extension. COSMO-CLM is able to reproduce the inter-annual variabilities of snow cover features as well as the

seasonal trend of snow cover duration and extension. Limitations emerge when the RCM simulates the progressive depletion of the snow cover in spring. Simulated snowmelt occurs faster than the observed one. Then, we investigate the influence of the spatial resolution of the climate model. The simulation at 0.0715° (about 8 km) is compared to a simulation performed at 0.125° (about 14 km). The comparison highlights the benefits provided by the higher spatial resolution in the accumulation season, reflecting the improvements obtained in temperature and precipitation fields.

Keywords COSMO-CLM · MODIS · Snow cover · Alps · Climate change · RCM

1 Introduction

Mountain areas have a high sensitivity to climate changes and they are often adopted as indicators of climate trends. The expected impacts will affect many fields of collective interest (Beniston 2003), including economic aspects related to winter tourism (Koenig and Abegg 1997; Elsasser and Bürki 2002; Agrawala et al. 2007; Scott and McBoyle 2007; Steiger and Mayer 2008) and hydropower production (Middelkoop et al. 2001; Christensen et al. 2004; Payne et al. 2004; Schaefli et al. 2007; Voigt et al. 2010) or social issues such as water resources (Barnett et al. 2005; Viviroli et al. 2007), ecosystem and biodiversity safeguard (Pauli et al. 1996; Theurillat and Guisan 2001; Walther et al. 2002; Keller et al. 2005; Jonas et al. 2008; Erschbamer et al. 2009). In the mountain environment, snow and ice play a key role for hydrology, ecosystem and climate. On the one hand, water accumulated in solid form rules the hydrology of mountain catchments and, consequently, it

✉ Pierfrancesco Da Ronco
   pierfrancesco.daronco@polimi.it

1   Department of Civil and Environmental Engineering,
    Politecnico di Milano, P.zza Leonardo da Vinci 32,
    20133 Milan, Italy

2   Regional Models and geo-Hydrological Impacts Division
    (REMHI), Centro Euro-Mediterraneo sui Cambiamenti
    Climatici, Via Maiorise, 81043 Capua, CE, Italy

3   Centro Italiano Ricerche Aerospaziali CIRA, Via Maiorise,
    81043 Capua, CE, Italy

affects the regime of the major rivers. On the other hand snow duration, distribution and spatial extent are determinant for human activities, vegetation and influence climate as feedback (Barnett et al. 1989; Cohen and Rind 1991; Hall 2004; Vavrus 2007; Fletcher et al. 2009). Focusing on the Mediterranean area, the Alps determine the water budget of a wide and populated region due to their geographic position in middle of the Europe. For example, in the Po river basin, the Alps contribute on average for about 50 % of the discharge that flows across the densely urbanised Po valley in northern Italy (Vanham 2012). Similarly, the Alpine area covers a significant percentage of Rhine, Rhone and Danube river basins and the snow accumulating in winter works as a natural regulator sustaining spring and summer streamflows. Furthermore, it is important to take into account that the Alpine region is one of the most studied mountainous areas of the world. It is characterized by complex climate features due to the interaction of different climates (Mediterranean, Continental, Atlantic and Polar) and to its complex topography (Frei et al. 2003; Beniston 2005). It turns out to be an area highly influenced by the effects of climate change that will affect, for example, the existence of glaciers and permafrost areas and, as consequence, the water cycle (Haeberli and Beniston 1998). For all these issues climate change projections for this region are a current major challenge and the impacts have become a major research topic in the last decades (Beniston 2003; Giorgi and Lionello 2008).

There is general agreement between Global Climate Models (GCMs) from the World Climate Research Programmes CMIP3 and CMIP5 (Meehl et al. 2007; Taylor et al. 2012) in predicting a future decrease in snow cover duration and maximum snow water equivalent in central Europe (Räisänen 2008; Brown and Mote 2009; Brutel-Vuilmet et al. 2013). However, snow cover sensitivity to precipitation and temperature changes is highly related to topographic features such as elevation, aspect and terrain shading. For example, snow duration at mid and low altitudes has shown to be more susceptible to temperature increases in the twentieth century (Laternser and Schneebeli 2003; Beniston et al. 2003a; Scherrer et al. 2004; Wielke et al. 2004; Hantel and Hirtl-Wielke 2007; Hantel and Maurer 2011). Similarly, climate projections in Alpine areas expect a reduction of maximum snow water equivalent (Beniston et al. 2003b; Martin and Etchevers 2005; Bavay et al. 2009; Brown and Mote 2009), changes in the accumulation timing (Beniston et al. 2003b; Bavay et al. 2009) and a shortening of the snow cover season (Beniston et al. 2003a) affecting especially mid and low elevations (see Gobiet et al. (2013) for an up-to-date review). This elevation dependence of snow cover response is certainly related to the altitudinal trends for temperature changes (Beniston and Rebetez 1996; Weber et al. 1997).

The elevation gradient of climate change in Europe is predicted by several studies that used GCMs or RCMs, from the pioneering research by Giorgi et al. (1997) to more recent investigations [e.g. López-Moreno et al. (2008), Im et al. (2010), Kotlarski et al. (2012)]. On the Alps, elevation varies significantly over short distances. Hence horizontal resolution becomes a determinant factor for simulating snow cover response to climate change over these complex mountain domains (Kunstmann and Stadler 2005; Dutra et al. 2011; Kotlarski et al. 2012; Steger et al. 2013).

Within the modeling framework, the offline coupling addresses this challenge forcing high-resolution land surface models by the outputs of GCMs or RCMs [e.g. Bavay et al. (2009); Magnusson et al. (2010)]. Statistic (Wilby et al. 1998) or dynamic (Giorgi et al. 2001) downscaling methods are involved to match the small scale of snow processes with that of climate models (Kunstmann and Stadler 2005; Fowler et al. 2007). However, the advantages provided by such a sophisticated modeling of snow physics remain highly affected by uncertainties introduced in the downscaling stage (Wood et al. 2004; Fowler et al. 2007). Furthermore the downscaled outputs may result physically inconsistent between themselves (Fowler et al. 2007), and the offline coupling may lead to land surface conditions inconsistent with the applied atmospheric inputs. In contrast, the simplified schemes of land surface implemented in the climate models have the advantage of ensuring consistency between parameters. Maps of snow covered area (SCA), Snow Cover Duration (SCD) and Snow Water Equivalent (SWE) obtained from the online coupling of RCMs and land modules are progressively regarded with more interest due to their increasing spatial resolution. Thus, the assessment of the outputs provided by limited area models for surface layers will become determinant for future climate studies.

Focusing on the snow processes, the evaluation should include the complete cycle of SWE from accumulation to snowmelt. Methods for distributing point measurements are required when one needs large-scale information on snow amounts (Elder et al. 1998; Foppa et al. 2007; Bavera and De Michele 2009). Interpolation introduces an additional source of errors especially where SWE measurements do not constitute a dense and extensive network. Maps of SWE based on passive microwave measurements from satellites (Chang et al. 1976; Rango et al. 1979; Clifford 2010) are available but the spatial resolution is lower than that allowed by the advances in regional climate modeling [e.g. ESA Globsnow SWE (Takala et al. 2011), AMSR-E/ Aqua Global SWE (Tedesco et al. 2004; Tedesco and Narvekar 2010)]. Moreover the accuracy of SWE retrieval algorithms based on passive microwaves is highly influenced by snow conditions and vegetation cover (Foster et al. 2005; Clifford 2010; Takala et al. 2011). Conversely, assessments of snow

duration and extension do not require data on the amounts of stored precipitation, thus allowing analysis through high-resolution satellite products using visible and near-infrared reflectance of snow (Dozier 1989). Binary maps (snow/not snow) are readily achievable from EO by several scientific devices (e.g. TM, ETM+, AVHRR, MODIS, MERIS) and methods (Gesell 1989; Ramsay 1998; Pepe et al. 2005; Frei et al. 2012; Dietz et al. 2012; Rittger et al. 2013). Accordingly, climatological indicators such as snow cover days (SCDs) and SCA are provided from catchment to continental scales (Gao et al. 2011; Foppa and Seiz 2012; Hüsler et al. 2014). In this context, the Moderate Resolution Imaging Spectroradiometers (MODIS) employed by polar-orbiting Terra and Aqua satellites provide the SCA product (Hall et al. 2002) with 500 m spatial resolution. MOD10A1 (Terra) and MYD10A1 (Aqua) contain daily tiles with a comprehensive observation of the study area per day. The high temporal resolution of the images (for example compared to that of Landsat and SPOT) allows to monitor daily fluctuations of SCA as response to observed temperature and precipitation. Such binary snow maps have been validated in many regions and under different conditions of land cover. Overall, they showed accuracy with reference to ground data over all seasons [for a review see Hall and Riggs (2007)]. Gap-filling procedures are available to estimate snow presence under clouds, preserving the temporal resolution of the product without significant losses of accuracy [e.g. Parajka and Blöschl (2008a), Gafurov and Bárdossy (2009), Hall et al. (2010), Paudel and Andersen (2011), Da Ronco and De Michele (2014)]. Besides the validation issues, the multiple applications of satellite snow products include data assimilation in Land Surface Models (LSMs) (Rodell and Houser 2004; Sun et al. 2004; Zaitchik and Rodell 2009).

Here, we firstly propose a validation methodology for RCM with respect to the simulation of snow duration and extension. The purpose is that of using signals and indicators of snow cover dynamics extracted from satellite products avoiding ground-based measurements. In our opinion, remote sensing datasets ensure some advantages when the processes are analysed at the regional scale. For example, on the Italian Alps few stations exist over 2000 m asl, while snow covers the ground until summer for altitude >3000 m asl. The assessment is based on 500 m-resolution remote sensing data. Here, the observational dataset is derived from MODIS binary snow products of MOD10A1 and MYD10A1. Cloud obstruction is removed by a recent procedure (Da Ronco and De Michele 2014) that has proved to be more accurate than other existing methodologies when applied to northern Italy. The high spatial and temporal resolution of these snow cover maps makes it possible to apply the same evaluation to different resolutions of the RCM and to different RCMs of the EURO-CORDEX project

(Kotlarski et al. 2014). However, the product is suitable for assessing snow cover simulations performed at high spatial resolution that can catch the topographic effects on climate dynamics (Montesarchio et al. 2014).

Then, we assess the reliability of snow cover outputs derived from the coupling of COSMO-CLM (Rockel et al. 2008) and TERRA_ML over the Po river basin, northern Italy. The non-hydrostatic limited area model COSMO-CLM was evaluated and used for simulating climate in the Alpine region using different spatial resolutions (Bucchignani et al. 2013; Haslinger et al. 2013; Feldmann et al. 2013; Montesarchio et al. 2014; Bucchignani et al. 2016). It was also run for predicting elevation gradients of climate change in Europe, including snow cover (Kotlarski et al. 2012). Recently, Klehmet et al. (2013) demonstrated the added value of COSMO-CLM hindcast with respect to SWE estimation from forcing NCEP-R1 reanalysis in Siberia. However, the assessment of the accuracy of COSMO-CLM snow cover outputs in the Alpine region is still missing.

We investigate also how the model resolution affects the reliability of snow cover simulations. Snow cover response is highly influenced by local topographic features such as slope, elevation and aspect. The elevation influences both accumulation and melting, being representative of average temperature, and the exposure to sunlight determines a different response of the areas facing north and south (Comola et al. 2015). Slope and concavity make an area more or less suitable to snow duration. The effects of these elements, that in mountain vary over short distances, can be simulated only with high spatial resolution. Recent studies by Montesarchio et al. (2014) and Bucchignani et al. (2016) have shown improvements in the simulated precipitation and temperature patterns over the Alpine space using a model setup with high spatial resolution [0.0715°and 0.125°, where the latter value is close to the highest resolution considered in the EURO-CORDEX project (Jacob et al. 2014)]. Snow cover simulations are expected to be improved by the better representation of topography. This point would highlight the added value of RCMs allowing more realistic simulations of climate dynamics over the Alps.

2 Case study: Po river basin and Italian alps

The Po is the major Italian river and one of the most important fluvial system in Europe. It flows more than 650 km eastward across northern Italy, draining 74×10^3 km^2. The basin area is located mostly in Italy, while minor fractions in Switzerland and France. Considering the level of utilization of water resources for agricultural and industrial purposes, the Po valley is the focal point of the Italian national economy. The Alpine region contributes for about 50 % of
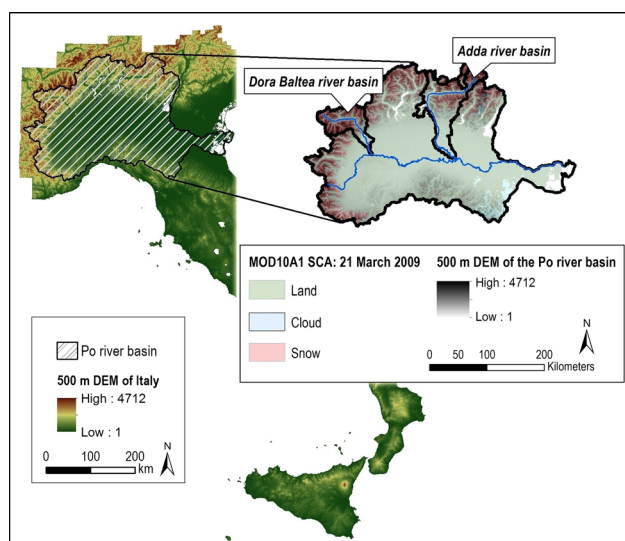
Fig. 1 Digital Elevation Model (DEM) of Italy at 500 m spatial resolution with the *contour line* of the Po river basin. The overlapped image shows the MODIS SCA product from Terra observation at the end of the 2008/2009 winter season, clipped over the basin boundaries. Original pixel classes have been reclassified to snow, land (not snow) and cloud (lack of information) before the application of the cloud removal procedure. The transparency allows to highlight the link between snow cover presence and altitude

its total discharge (Vanham 2012). Focusing on the topographic features of the basin, the tributaries of the Po river collect water from mountain regions that reach altitudes over 4500 m asl (Fig. 1). About 30 % of the area lies above 1000 m asl, where snow dynamics play an important role in the hydrologic cycle. A recent study (Da Ronco and De Michele 2014) showed that the SCA fluctuates from a percentage higher than 30 % of the entire basin in the middle of the winter to 5 % in spring. This value reduces to <1 % in summer, where snow is found only over glaciers in Lombardia, Piemonte and Valle d'Aosta regions. The analysis was carried out starting from remote sensing images.

Thus, the spatial and temporal evolution of the snow cover over the basin is a core issue for characterizing the hydrologic regime of the river, as well as for assessing its susceptibility to changing climatic conditions.

3 Datasets

3.1 MODIS snow covered area maps

MODIS is the Spectroradiometer on board Terra and Aqua satellites and provides powerful data for studying the Earth system. MODIS products include MOD10A1, a set of daily data available from February 2000 that contains snow maps from the Terra satellite. Similarly, MYD10A1 are

products derived from the MODIS on board the Aqua satellite, launched in May 2002. MOD10A1 and MYD10A1 contain daily snow albedo (Klein and Stroeve 2002), fractional snow cover (FSC) (Salomonson and Appel 2004, 2006) and the snow cover daily tiles (SCA). The latter are binary maps (snow/not snow) (Fig. 1), named SCA, available in the National Snow and Ice Data Center (NSIDC). Here, we used SCA maps which belong to Collection 5 of MODIS snow products (Riggs et al. 2006). In MOD10A1/MYD10A1 SCA, cloud masks are derived from MOD35, with daily temporal and 1 km spatial resolution. Each pixel not masked by clouds is processed by the snow mapping algorithm SNOMAP (Hall et al. 2001) which performs tests to identify snow in the image. SNOMAP involves a grouped-criteria technique which uses the Normalized Difference Snow Index, (NDSI), and other spectral threshold tests (Hall et al. 1995, 2001; Klein et al. 1998). Our choice of adopting the binary product, instead of the fractional one, is due to its wider use in the last decade, that led to numerous assessments of its reliability (Hall and Riggs 2007). On the Alps, a comprehensive assessment for Aqua and Terra products was provided by Parajka and Blöschl (2006) for Austria. That validation area presents similarities with our study region, which adjoins Austria for a small part. In Europe, another recent evaluation in the French Pyrenees is reported in Gascoin et al. (2015). Considering the good performances shown by MYD10A1/MOD10A1 in all the cases, these MODIS datasets seem ready to be used as reference observations for assessing RCM simulations. The value of MODIS SCA data is confirmed by their wide use in hydrology and climate studies, including data assimilation in Land Surface Models (LSMs) (Rodell and Houser 2004; Zaitchik and Rodell 2009).

3.2 Cloud-reduced and cloud-free snow cover maps

MOD10A1 and MYD10A1 snow cover daily tiles present a cloud coverage. As consequence, the temporal resolution of the data reduces. Several procedures have been proposed for mapping snow despite cloud obstruction (Parajka and Blöschl 2008a; Gafurov and Bárdossy 2009; Parajka et al. 2010; Paudel and Andersen 2011). Methods are based on spatio-temporal combinations of MODIS data and in some cases they allow a reconstruction of snow cover with an accuracy comparable to that of the source product [see Chang and Hong (2012) for a review]. Recently, Da Ronco and De Michele (2014) proposed an innovative solution for cloud gap-filling descending from the adaptation and combination of previous methodologies. First, the procedure involves conservative temporal filters and a spatial filter based on the snowline elevation (Parajka et al. 2010). Remaining clouds are basically processed by a 6-day backward temporal filter, which classifies each cloud cell on

the basis of its most recent observations within the previous week. A seasonal filter intervenes for assessing snow presence where clouds cover the same area for more than 1 week. The final product consists of 10 years (2003–2012) of cloud-free daily maps of snow cover, suitable for hydrologic and climate studies. The compromise to accept for having cloud-free images is a reduction of the reliability of the observational dataset. However, this solution showed higher accuracy for daily snow mapping on the Italian Alps when compared to previous techniques. The detailed validation of the cloud removal procedure can be found in Da Ronco and De Michele (2014). The average decrease of accuracy from the source MOD10A1 SCA map to the cloud-free product is about 4 %. The bias was computed at the pixel scale on more than 40 validation days. Considering that underestimation and overestimation errors balance in the gap-filling steps, the variables computed at the basin scale, such as the snow cover fraction (SCF), are expected to maintain a reliability even higher than that ensured for a given cell. To have an additional confirmation that the procedure does not influence the results of the comparison, some of the analyses will be repeated basing on the outputs of the first step of the cloud removal. The first step of the procedure (Step 1) combines Aqua and Terra images of the same day and it reduces the cloud mask taking advantage from these two available observations (i.e. a certain area may be cloud covered at the Terra overpass, but cloud-free few hours later, when Aqua overpasses the region). Thus, assuming that Aqua and Terra SCA have the same accuracy, Step 1 does not decrease the reliability of the observational dataset. The limitation is that the reduced cloud masks are still very intrusive after Step 1 and it is not possible to derive information such as the snow cover days per year. However, the snow cover fraction can be computed considering, for example, those days having <5 % cloud coverage after Step 1. The threshold imposed to the cloud percentage is necessary. In fact, when the satellite field of view is mostly obstructed, it is likely that clouds are not distributed homogeneously over snow free and snow covered areas. This could lead to an erroneous estimation of the snow cover fraction as it is computed as the ratio between snow covered area and total cloud-free area.

3.3 Snow cover maps from COSMO-CLM

The regional climate simulation has been carried out with COSMO-CLM (Rockel et al. 2008), in the configuration optimized at CMCC (Bucchignani et al. 2016). COSMO-CLM is a non-hydrostatic regional model developed by the CLM Community. It is the climate version of COSMO-LM weather model (Steppeler et al. 2003), initially developed by the Deutscher Wetterdienst (DWD) and then by the Consortium for Small-scale Modeling (COSMO). Thanks to its

Table 1 Main features of COSMO-CLM simulation setup

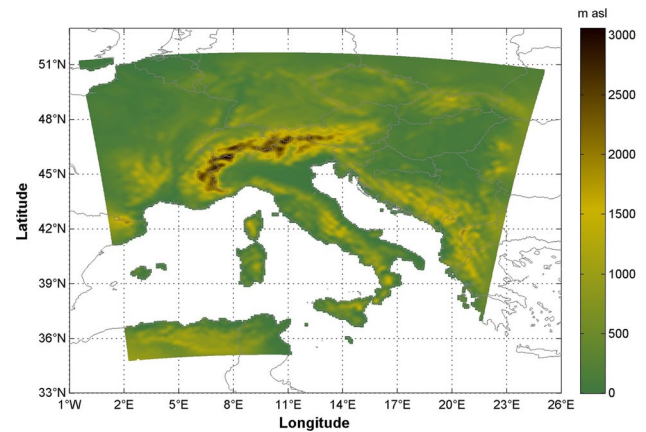| COSMO-CLM version	4.8_clm19
Horizontal resolution	0.0715°
Number of vertical levels	40
Soil model	TERRA_ML
Number of soil levels	7
Integration scheme	Runge-Kutta, 3rd order
Time step	40 sec
Convection scheme	Tiedtke (1989)

Fig. 2 Orography of the computational domain of simulation used in COSMO-CLM runs. A mesh of 224×230 points with the resolution of 0.0715° is adopted. The physical domain, where the results can be considered significant, is obtained from the computational domain excluding the relaxation zone (15 grid points from each boundary)

non-hydrostatic formulation, COSMO-CLM can be used to perform simulations at a very high horizontal resolution (between 1 and 50 km), allowing a better representation of subgrid scale physical processes and convective phenomena (Doms et al. 2011). From a mathematical point of view, the Navier-Stokes equations are used to express the atmospheric physical laws. In addition, several parameterizations are included to consider phenomena taking place on unresolved motion scales (Doms et al. 2011). From a numerical point of view, the integration method is the Runge-Kutta scheme. It is worth noting that, in the framework of PRUDENCE (Christensen and Christensen 2007) and CORDEX (Giorgi et al. 2009) projects, COSMO-CLM has revealed a good capability in reproducing the mean climate properties of the analyzed areas, providing similar results to those shown by the other RCMs involved (Table 1).

The simulation analyzed here has been carried out by using as initial and boundary conditions the ERA-Interim Reanalysis (Dee et al. 2011), produced by the European Centre for Medium-Range Weather Forecasts (ECMWF). In this way, the model performances have been evaluated

in "perfect boundary conditions", so that only the uncertainties related to the RCM have been taken into account, avoiding those introduced by the usage of a global climate model outputs as initial and boundary conditions. The entire control simulated period is 1979–2011, but the temporal window considered for the analyses is 2003–2011. This is due to the need to fit the temporal coverage of the cloud-free dataset of snow cover (2003–2012) used to perform the comparison with the regional model output. So, the model results are not influenced by initial conditions. The horizontal resolution adopted is 0.0715° (about 8 km) and the simulated domain covers the whole Italian peninsula (Fig. 2). The dataset used to compute the orography in COSMO-CLM is the Global Land One-kilometer Base Elevation (GLOBE, http://www.ngdc.noaa.gov/mgg/topo/globe.html), provided by the National Geophysical Data Center. It includes the orographic height of the global land surface at a resolution of 30 arc seconds (about 1 km). The orographic value for each COSMO-CLM grid point of a specific area of interest at the required resolution is then generated by performing an average of the values reported in the GLOBE dataset. More details about the main characteristics of COSMO-CLM and the setup used to perform the simulation are described in Bucchignani et al. (2016).

Land-surface interactions in COSMO-CLM are modeled by the soil model TERRA_ML (Grasselt et al. 2008), whose aim is to calculate temperature and specific humidity at the ground, solving equations describing thermal and hydrological budgets (Davin et al. 2011). Hydrological processes are modeled through various interactive reservoirs of water at the surface and in the soil to predict the liquid water stored. At each time-step, and for each cell, the mass balance is solved in the storages. Water accumulates in the interception reservoir (which contains all surface water including dew on plants and on the soil), in the snow reservoir (containing snow but also frozen surface water and rime) and in the seven soil layers. Reservoirs communicate via infiltration, percolation and capillary movements. Even melting of snow and freezing of water in the interception reservoir displace water content from a storage to another. Focusing on the snow module, the snow reservoir is fed by snow coming from the lowest atmospheric layer and rime from the interception reservoir. Water leaves in the form of evaporation or snowmelt. The latter either infiltrates or slips as surface runoff, depending on the soil water content. The water budget per unit area within the snow layer reads as

$$\rho_w \frac{dW_s}{dt} = P_s - E_s - I_s - R_s \tag{1}$$

where ρ_w (kg/m^3) is the density of water, W_s (m) is the snow water equivalent, E_s [kg/(m^{2}s)] is the evaporation from the snow reservoir, P_s [kg/(m^{2}s)] is the precipitation rate of snow, I_s [kg/(m^{2}s)] is the infiltration into the soil

and R_s [kg/(m^{2}s)] is surface runoff. I_s and R_s come from snowmelt. Here, only P_s works as input from the atmospheric part of the model. All the other variables are calculated within the context of the snow module in TERRA_ML. Several snow cover features (e.g. average density, depth, surface temperature, albedo) are provided as outputs. In this study we look for the binary information about snow cover presence. With this aim each calculation unit is identified as snow covered whenever the modelled SWE is >1 cm.

A more detailed description of this module and of the physical parameterizations used in COSMO-CLM are reported in Doms et al. (2011).

4 Methods

Here, we propose a methodology to extract information about snow cover duration and extension from MODIS SCA maps and we compare these with the RCM outputs, avoiding ground-based data. MODIS data are appropriate to perform these analyses as their spatial resolution (500 m) is higher than the one used to carry out state-of-art regional climate simulations.

4.1 Snow cover extent

During the year, the basin experiences a relative SCA, SCF (Snow Cover Fraction), which ranges from the surface of glaciers ($SCF \simeq 0$) to the entire domain ($SCF = 1$). In regions with complex topography, the variability of snow cover dynamics over horizontal distances is certainly smaller than that caused by altitude. Reporting the information on snow cover presence on a Digital Elevation Model (DEM), the fraction of area covered by snow can be computed either for the entire basin or per altitude range classes (ARCs). Hence, observed $SCF(t, z_1 \leq z < z_2)$ will provide the SCA at a certain time t and for the zone between the elevations z_1 and z_2. The time dependence of $SCF(z_1 \leq z < z_2)$ across the melting season represents the depletion curve (Schaper et al. 1999; Brander et al. 2000; Seidel and Martinec 2002, 2004). Referring to remote sensing snow products, snow depletion curves were used for snowmelt-runoff forecasting purposes since the timing of the processes can be inferred [e.g. Rango et al. (2003), Lee et al. (2005), Parajka and Blöschl (2008b)]. In assessing snow cover simulations driven by RCM, the time series of SCF is derived from both MODIS images and RCM simulations. A comparative study can be performed using observed and simulated accumulation timings and depletion curves. Over the year, sudden increases of SCF reflect extensive snowfall within the basin. In contrast, SCF gently decreases in the melting season due to the increasing

temperatures. The slope of each depletion curve, $\frac{dSCF}{dt}$, is directly linked to large-scale melting rates. In the RCM snow simulations it will indirectly reflect/affect temperature bias in spring.

The main limitation in comparing simulated and observed values of *SCF* at the basin scale is that the maps may present similar snow cover extent but inconsistent snow distribution.

4.2 Altitudinal distribution of snow covered areas

Snow cover dependence on altitude can be inferred coupling snow cover maps with a DEM having the same spatial resolution. Thus, each cell contains a double information on snow presence and elevation. We define the snowline as the average elevation of snow covered areas (Parajka and Blöschl 2008a; Da Ronco and De Michele 2014). The snowline has important impacts on the ecosystem, since its annual trend reflects snow persistence at mid and low elevations (Hantel and Maurer 2011; Hantel et al. 2012). Its altitude is suddenly lowered by wide snowfalls during the accumulation season, while it increases progressively in spring and summer. The temporal variability of the snowline during the melting season is a concise information about the rate of snow cover depletion. The snowline is calculated from both MODIS SCA and RCM-derived snow cover maps. The comparison would provide an indication of RCM performance in simulating snow cover distribution over altitudes and its inter-annual variability. MODIS snow cover maps are matched with the DEM used in the cloud removal procedure (Da Ronco and De Michele 2014), having 500 m resolution. On the other hand, the source dataset used to compute the orography in COSMO-CLM is the Global Land One-kilometer Base Elevation (GLOBE, spatial resolution of about 1 km), provided by the National Geophysical Data Center. The RCM computes the elevation of the calculation grid points at the required resolution by performing an average of the values reported in the GLOBE dataset. This information can be coupled with that on snow cover presence for the same point at each calculation time-step.

4.3 Snow cover duration

For a given location, snow cover duration indicates the number of days with snow at the ground. This variable is highly influenced by local topographic features such as aspect, slope and shadow. However, the altitude becomes the driving factor increasing the spatial scale of observation. The duration of snow cover will be quantified globally over the area of interest using the snow duration curves, and locally using the snow duration maps.

4.3.1 Snow cover duration curves

For a chosen domain, the snow cover duration curve is defined as the fraction of the year in which snow covers an area equal or greater than a certain value. We calculate it as the complement of the cumulative distribution function (cdf) of the daily SCA. Given a reference year, let n_y indicate the total number of observations and n_d the number of days with $SCF < scf$. One can easily evaluate the exceedance frequency

$$\bar{F}(scf) = 1 - \frac{n_d}{n_y} \tag{2}$$

Daily percentages of SCA, the observed values of *SCF*, are computed by dividing the number of pixels classified as snow by the whole number of pixels within the domain. The frequency $\bar{F}$ decreases while increasing *scf*. The snow duration curve is the plot of $\bar{F}$ versus *scf*. The value of this graph descends from the joint information of snow extension and duration. In our opinion, the snow cover duration curve can be seen as a signature of a certain region reflecting its topographic and climatic features at regional scale. However, it does not contain any information on the timing of the processes. The snow duration curve simulated by RCMs can fit the observed one even though the time series of *SCF* are inconsistent.

4.3.2 Snow cover duration maps

The snow cover duration map (Brander et al. 2000; Seidel and Martinec 2002; Tong et al. 2009; Gao et al. 2011; Foppa and Seiz 2012; Hüsler et al. 2014) consists of gridded values of snow cover days (SCDs) per calendar year, per hydrologic year, or per season. It maintains the same spatial resolution of the source satellite product since a binary information on snow presence is available pixel by pixel. Each cell is thus associated with a value that represents the number of days with snow cover, ranging from 0 to 365/366. Using MODIS data, Foppa and Seiz (2012) derived such maps for Switzerland and provided a quantitative evaluation in comparison to three in-situ snow observation sites representing different climatological regimes. An example of MODIS-derived snow cover duration map is included in Fig. 3 for the Po river basin. Here, the application of a cloud removal procedure becomes determinant for assessing the number of days with snow at the ground. Snow cover days are provided even by the RCMs, computing the number of days with simulated snow depth higher than a certain threshold. The value of this map for assessing RCM snow cover simulations descends from the local scale of the information, which allows to investigate in detail particular areas such as those surrounded by mountains but located at low altitude. There, the model is asked
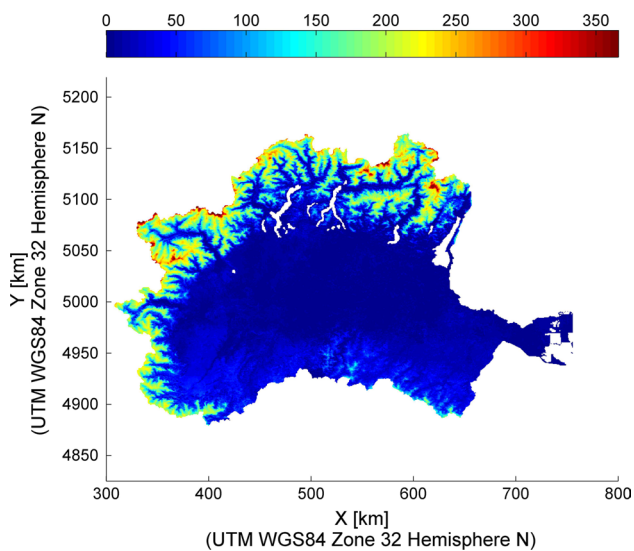
Fig. 3 Example of snow cover duration map for year 2004, derived from MODIS SCA product for the Po river basin. Each pixel is associated with an integer value ranging from 0 to 365/366 (snow cover days)

to reproduce physical processes whose forcings vary significantly over small distances due to the prominent elevation gradient.

In order to compare the model outputs with MODIS observations, it is necessary to remap the data on a common grid. In this study, as already performed in Kotlarski et al. (2014), the coarser grid has been used as reference; so, MODIS SCDs have been upscaled to the COSMO-CLM grid. In this way, a value of snow cover duration derived

from observations is associated to each RCM spatial unit and it can be compared against simulated SCDs. The resampling can be performed with different techniques. Exploiting the standard tools for spatial analysis, it is possible to apply a bilinear resampling to the MODIS-derived snow cover duration maps. However, this resampling method excludes a high number of cells belonging to the source map from the computation that produces the 8 km grid values. Thus, we preferred to produce resampled snow cover duration maps where each 8 km cell contains the average value of snow cover duration of its nearest 256 (500 m) cells. If some of these cells lie outside the basin boundaries, the mean value is computed exploiting only the elements inside.

5 Results

The RCM is run at 0.0715° resolution. Precipitation and temperature fields at this resolution were recently produced, showing improvements with respect to 0.125° simulation (Montesarchio et al. 2014; Bucchignani et al. 2016). A comparative study between snow cover simulations performed at different model resolutions has been carried out. The target is the investigation of the benefits provided by a better representation of the Alpine orography in regional climate simulations.

Altitude is the key topographic element affecting snow cover dynamic since it strongly influences temperature and precipitation. In Figs. 4 and 5, we provide a comparison between the orography used in the climate simulation and that exploited in the processing of satellite observations. The latter comes from a 8 km resampling of the 500 m DEM
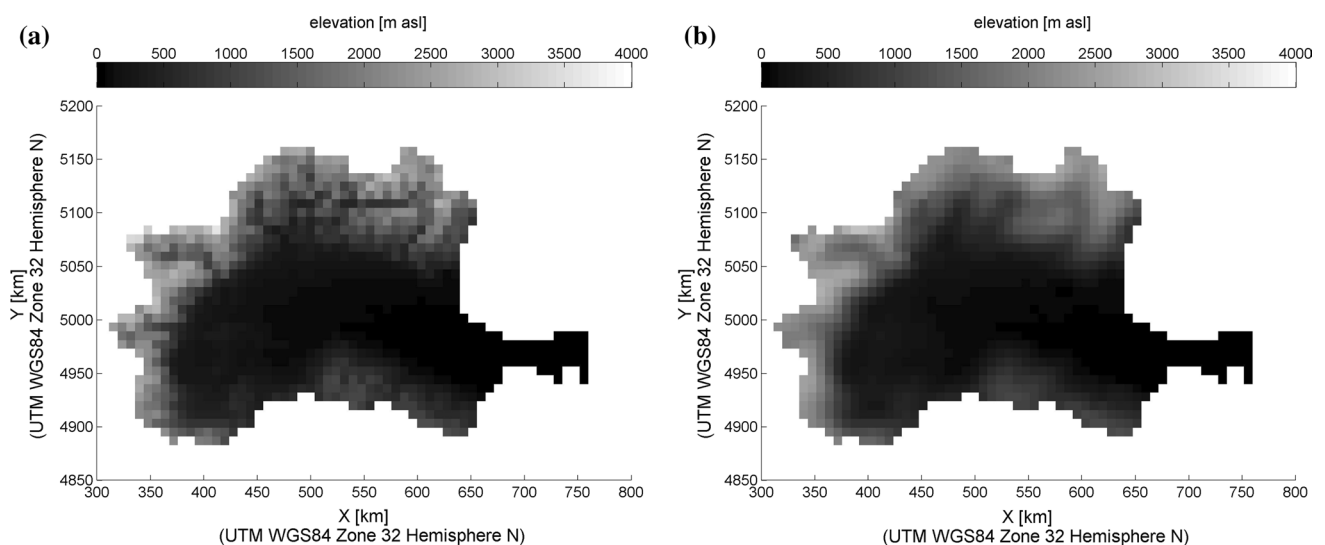

Fig. 4 Comparison between the 8 km resampling of the 500 m DEM (**a**) and the orography generated by COSMO-CLM for the 8 km simulation over the study domain (**b**). **a** 8 km resampled DEM. **b** CCLM orography
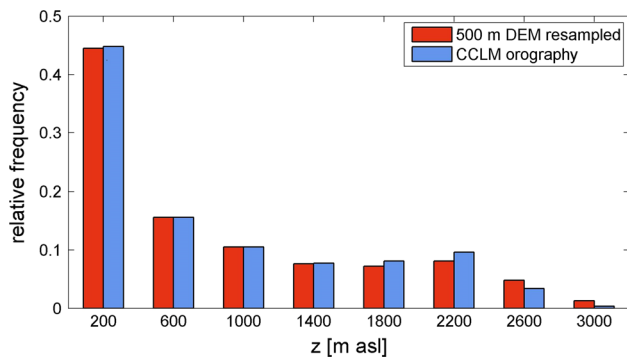
Fig. 5 Altitudinal distribution of the cells in COSMO-CLM orography and in the 8 km resampled DEM. The x-axis label represents the elevation in the middle of the equal 400 m intervals

which supported the steps of the cloud removal procedure. The gap between 500 m and 8 km resolutions is important. Therefore, we matched each cell of 8 km COSMO-CLM orography with its nearest 256 pixels of the 500 m DEM. The location of each cell is identified by its centroid, whose coordinates are given in UTM WGS84 in both maps. Then, the average values are delivered to the altitudes of the new grid cells. From Fig. 5 one might state that the distribution of the pixels over altitude is quite similar considering the entire basin. However, the spatial information found in Fig. 4 shows that in the tight and lengthened valleys, such as the Dora Baltea and Adda river basins (see Fig. 1 for the spatial location of such areas), the orography of COSMO-CLM is more regular with lower differences between the altitude of ridges and valleys. Moreover, COSMO-CLM

Fig. 6 Comparison between observed (cloud-free MODIS SCA product) and simulated (COSMO-CLM 8 km) daily (−) and average monthly (−◦−) values of Snow Cover Fraction for the Po river basin over the period January 2003–December 2011
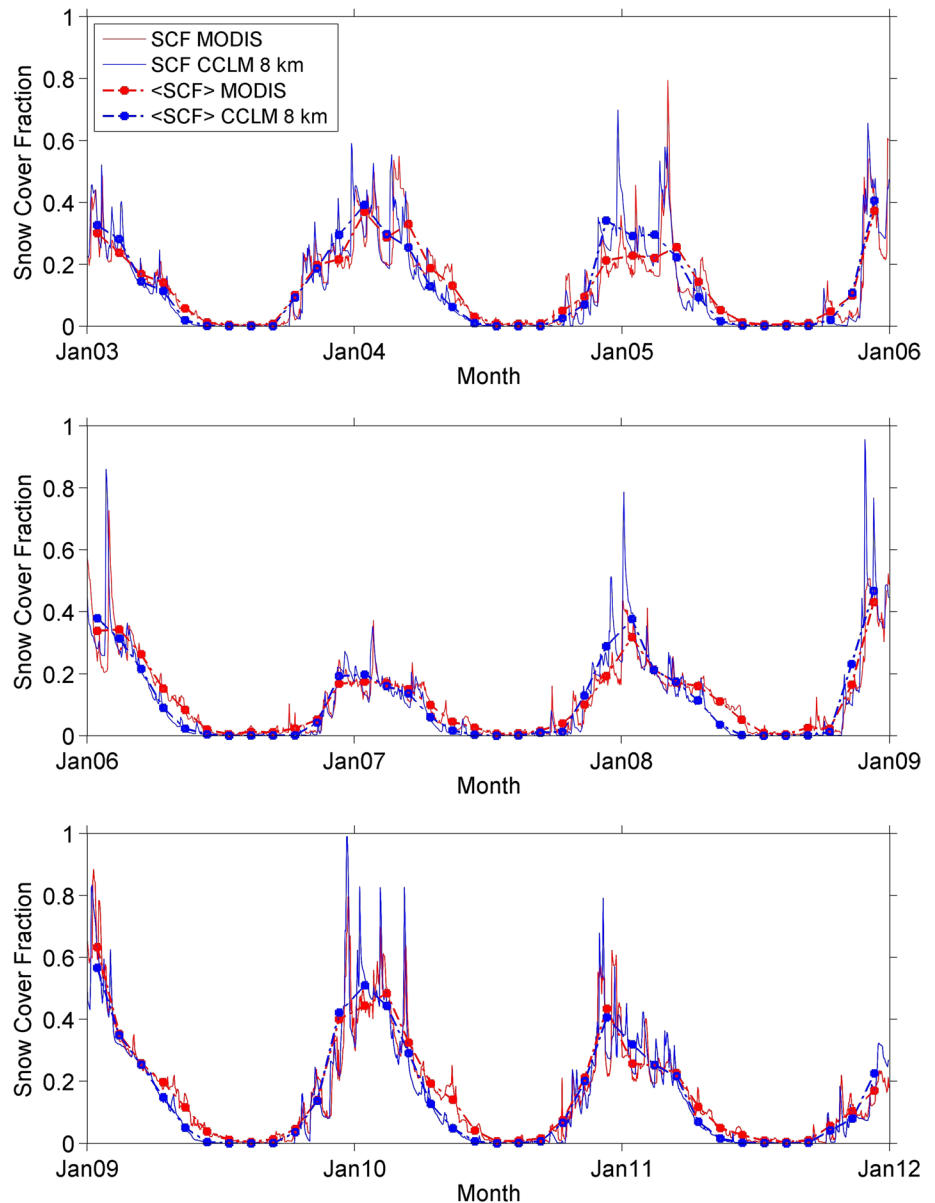
orography presents a smaller number of pixels over 2500 m asl and its highest value remains below 3100 m asl (the 8 km resampled DEM reaches 3600 m asl). These differences could influence the results of snowpack simulation entailing lower differences between cells when compared to that derived from MODIS data.

5.1 Simulation results with COSMO-CLM at resolution 0.0715°

5.1.1 Snow cover extent

The temporal behavior of SCF is shown in Fig. 6 for 9 years. We report observed and simulated daily and average

monthly values of SCF. It is possible to notice the inter-annual changes in the trend of the snow extent. Overall, the seasonal variability of SCF is well reproduced by the COSMO-CLM simulation. Systematic disagreements affect the melting season, when the simulated snow cover disappears faster. In the depletion phase, the spatial resolution becomes determinant since snow extent reduces progressively, approaching zero in the late spring. While from the satellites we can observe directly an area with altitude over 4700 m asl computing a snow cover fraction >0 over all the year, the elevation of the nearest COSMO-CLM cell is more similar to the average altitude of several snow-free MODIS cells. The simulation of the physical processes is expected to reproduce the average condition of
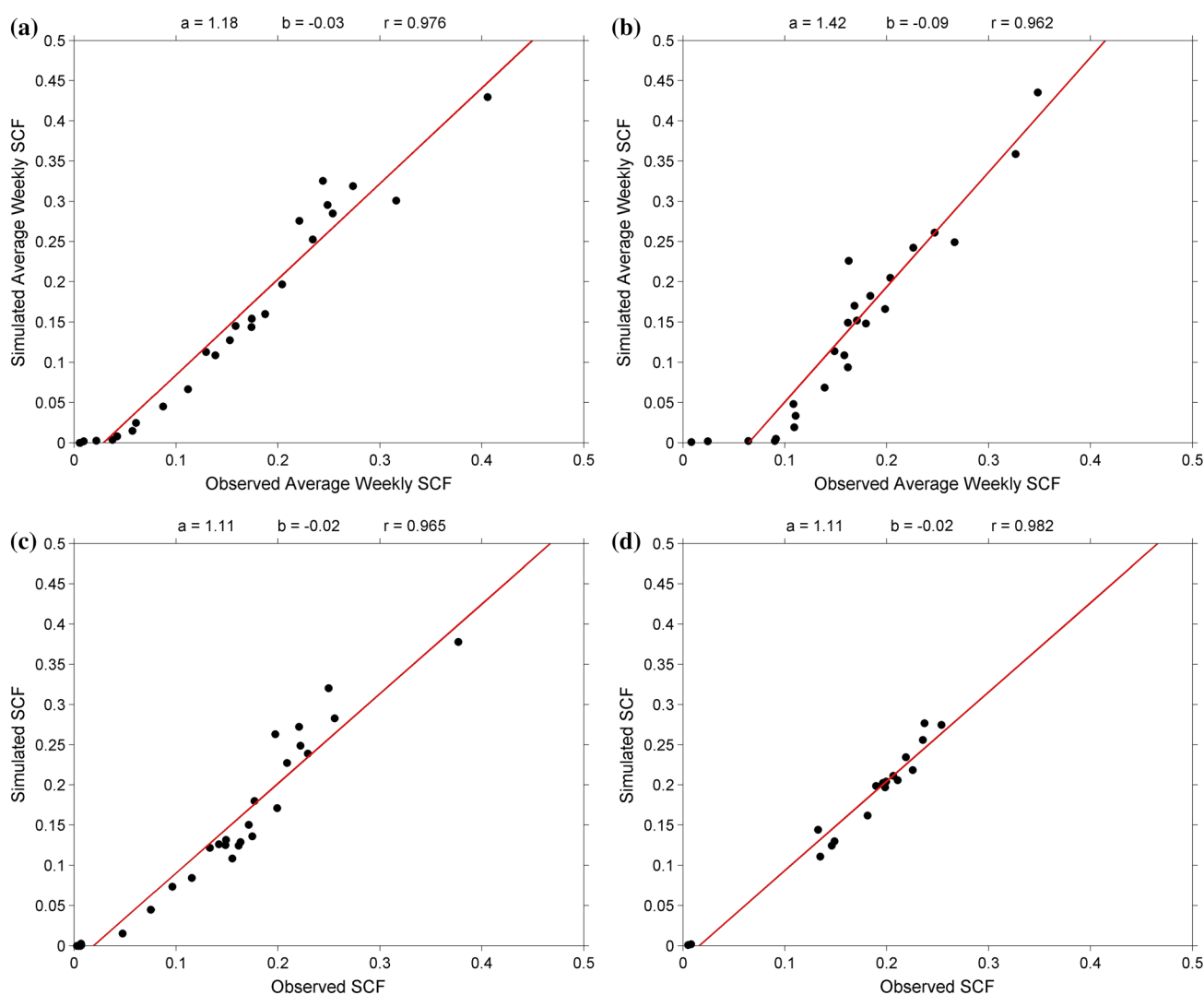

Fig. 7 Observed [cloud-free MODIS SCA product (**a**, **b**) and basic combination of Aqua and Terra data (**c**, **d**)] versus simulated (COSMO-CLM 8 km) average weekly values of Snow Cover Fraction for the Po river basin. The *straight line* $y = a \cdot x + b$ is found by linear regression. The panels report even the Pearson r coefficient. Period January–June of year 2003 (**a**, **c**) and 2008 (**b**, **d**). **a** Cloud-free, 2003, **b** Cloud-free, 2008. **c** Step 1, 2003. **d** Step 1, 2008

the calculation unit. Thus, the simulation at 8 km resolution is subjected to this limitation when compared with the high-resolution MODIS maps. In winter, average monthly SCA is well reproduced by COSMO-CLM for most of the testing years. Overestimation affects especially 2004/2005 and 2007/2008 accumulation months. Increasing the scale of observation, the evaluation of the simulation of daily *SCF* should take into account that our observational dataset is the result of spatial and temporal filtering of MODIS images for cloud removal. In particular, extensive snowfalls may be observed with a few days of delay. With respect to this evidence, peak timings seem rightly captured for all the study period. During the accumulation season, daily snow cover extents are usually overestimated. Since peaks are the results of wide snowfalls within the domain, causes of disagreement should be sought in temperature and precipitation bias.

Figure 7 reports the relationship between observed and simulated average weekly values of *SCF* from January to the end of June for 2003 and 2008. Beyond the observed and the simulated series of the average weekly *SCF*, $SCF_{obs,i}$ and $SCF_{sim,i}$, in Fig. 7, we report the coefficients of the straight line that best fits the data, $y = a \cdot x + b$, found using the method of least squares. The Pearson correlation coefficient (r) is given as well. In case of perfect agreement, the linear regression returns $a = 1$, $b = 0$ and $r = 1$ (Krause et al. 2005). Note that values of $a > 1$, found for all the years, suggest that the model systematically overestimates the difference between higher (winter) *SCFs* and smaller (spring) *SCFs* in the analysed temporal window. Focusing on the lower *SCF* values, it appears clearly that COSMO-CLM underpredicts the SCA in spring. The comparison for the entire study period is provided in Table 2 considering the first half-year as a whole (January–June)

and the melting season of each year (March–June). There, we report the Nash-Sutcliffe efficiency index (Nash and Sutcliffe 1970), *NSE*, and the values of the root mean square error, *RMSE* (Chai and Draxler 2014). *NSE* is expressed as

$$NSE = 1 - \frac{\sum_{i=1}^{n}(SCF_{obs,i} - SCF_{sim,i})^2}{\sum_{i=1}^{n}(SCF_{obs,i} - \overline{SCF}_{obs})^2} \qquad (3)$$

and ranges between 1 (perfect fit) and $-\infty$. If the efficiency is lower than zero, it indicates that the mean value of the observed time series is a better predictor than the model. The values of *NSE* in Table 2 demonstrate that COSMO-CLM always beats the mean of the observed time series.

The same test is then repeated using snow cover maps having <5 % cloud coverage after being processed by Step 1 of the gap-filling procedure, which combines Aqua and Terra data to get a cloud-reduced image. The results confirm what found using the cloud-free snow maps as observational dataset, even if the sample size is lower and usually composed of several continuous days of clear-sky [Fig. 7 panel (c) and panel (d)]. For this reason, we consider this second comparison less reliable than the first one for assessing model performances.

5.1.2 Snow depletion curves

The snow depletion curves shows the progressive disappearance of the snow cover in spring. The temporal variability of $SCF(t, z_1 \leq z < z_2)$ is reported for two altitude bands ($500 \leq z < 1500$ and $z \geq 1500$ m asl) using its daily and average weekly values. The separation of the domain in different altitude range classes (ARCs) can highlight whether the bias found for *SCF* is mainly due to the

Table 2 Values of *NSE* and *RMSE* from the comparison of observed (cloud-free "CF" and cloud-reduced "Step 1" MODIS SCA) and simulated values of *SCF*

Year	CF: Mar–Jun		CF: Jan–Jun		Step 1: Jan–Jun		
	NSE	*RMSE*	*NSE*	*RMSE*	*NSE*	*RMSE*	N_D
2003	0.83	0.02	0.89	0.04	0.89	0.03	29
2004	0.75	0.05	0.78	0.06	0.89	0.06	18
2005	0.89	0.04	0.77	0.06	0.72	0.05	35
2006	0.74	0.05	0.76	0.07	0.85	0.08	18
2007	0.72	0.03	0.80	0.03	0.77	0.03	21
2008	0.15	0.05	0.61	0.06	0.98	0.02	19
2009	0.73	0.04	0.93	0.05	0.96	0.04	18
2010	0.59	0.06	0.82	0.07	0.86	0.06	8
2011	0.79	0.03	0.82	0.05	0.92	0.03	29

When the reference dataset is composed of cloud-free maps, the comparison between the average weekly *SCF* is provided. The last three columns are related to the comparison between simulated and observed daily *SCF*, where the reference SCA is computed using Aqua and Terra maps processed by Step 1 of the cloud removal procedure (Da Ronco and De Michele 2014). Only those images with remaining cloud cover percentage lower than 5 % are exploited, whose amount is reported in the field N_D
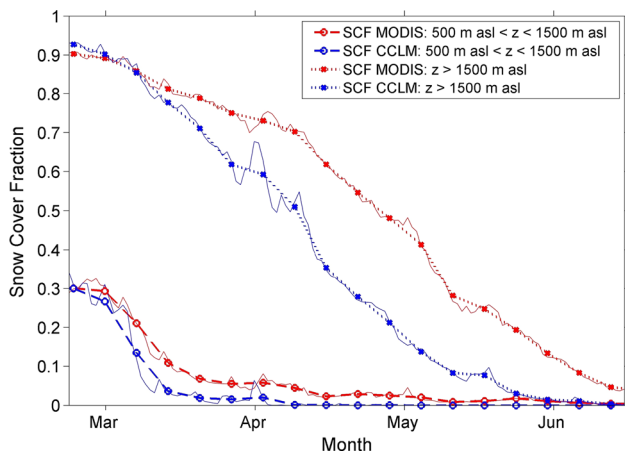
Fig. 8 Comparison between observed (cloud-free MODIS SCA product) and simulated (COSMO-CLM 8 km) average snow depletion curves for two altitude ranges (between 500 and 1500 m asl and above 1500 m asl). The daily (−) and average weekly (−∘−/−×−) values of Snow Cover Fraction are computed for each day (or week) as mean over the 9 year sample (2003–2011)

mountainous part of the basin or to the middle altitudes. RCM performances in snow cover simulation may depend on altitude, as shown in Steger et al. (2013).

Instead of reporting the model performances for all the years separately, we grouped the 9 curves using the average values obtained for a given date, or a given week, in the period 2003–2011 (Fig. 8). The simulated depletion rate is clearly overestimated for both ARCs. A slight overestimation of *SCF* exists only in the late winter for the area above 1500 m asl. Focusing on the higher altitude band, COSMO-CLM snow cover extent reduces to less than half of the observed after April. The relative error increases accordingly. The snow cover disappears before June, when remote sensing observations still detect a not-negligible snow covered area. Here, the spatial resolution is determinant for reproducing the orographic effects on snow cover patterns. For altitudes below 1500 m asl snowmelt completes before April, while in the MODIS images snow lasts for at least 1 month later. Considering each year individually, we found that the underestimation of *SCF* affects all springs. The individual figures are not reported for brevity.

5.1.3 Snow cover distribution

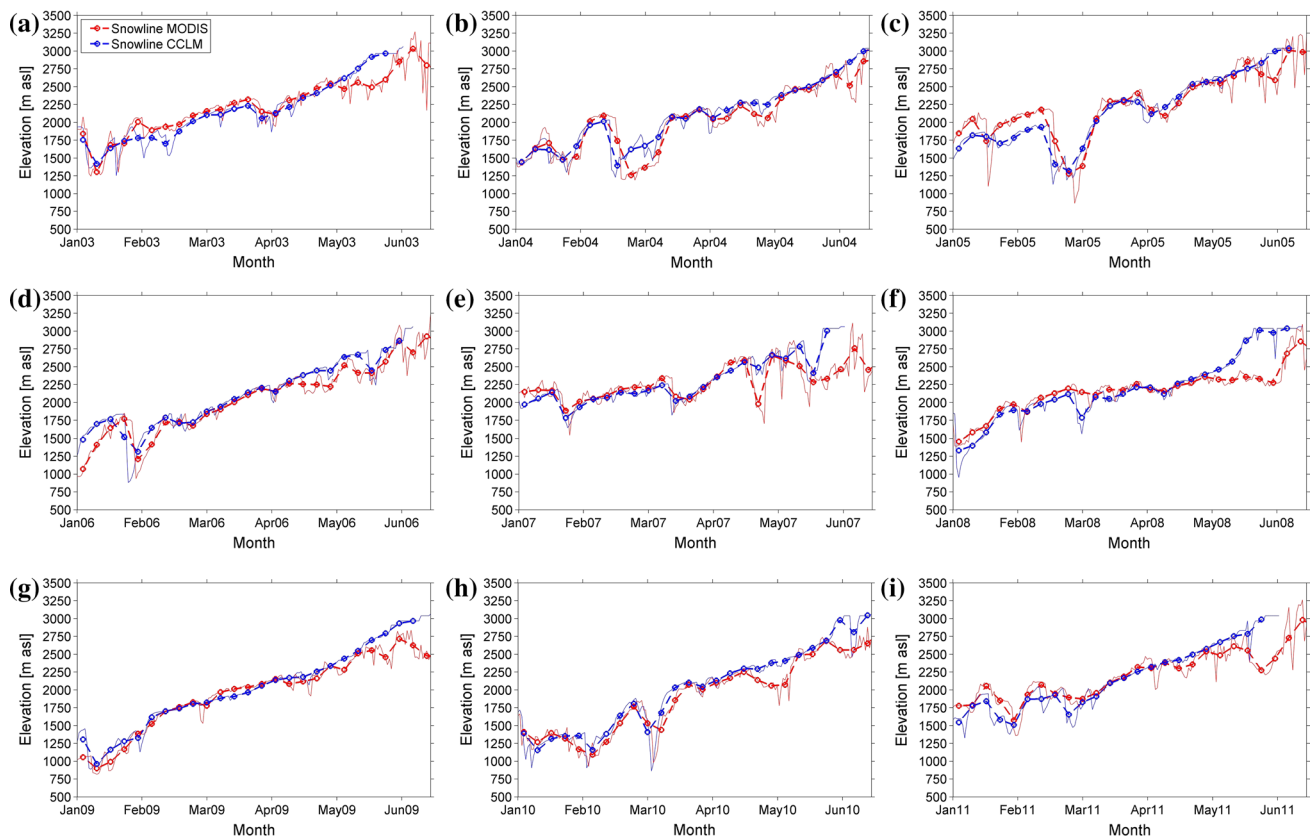The temporal variability of the snowline along the year is represented in Fig. 9, where the average altitude of SCAs

Fig. 9 Comparison between observed (cloud-free MODIS SCA product) and simulated (COSMO-CLM 8 km) snow lines for each year. Both the daily (−) and average weekly (−∘−) values of the mean altitude of snow covered areas are shown. **a** 2003, **b** 2004, **c** 2005, **d** 2006, **e** 2007, **f** 2008, **g** 2009, **h** 2010, **i** 2011
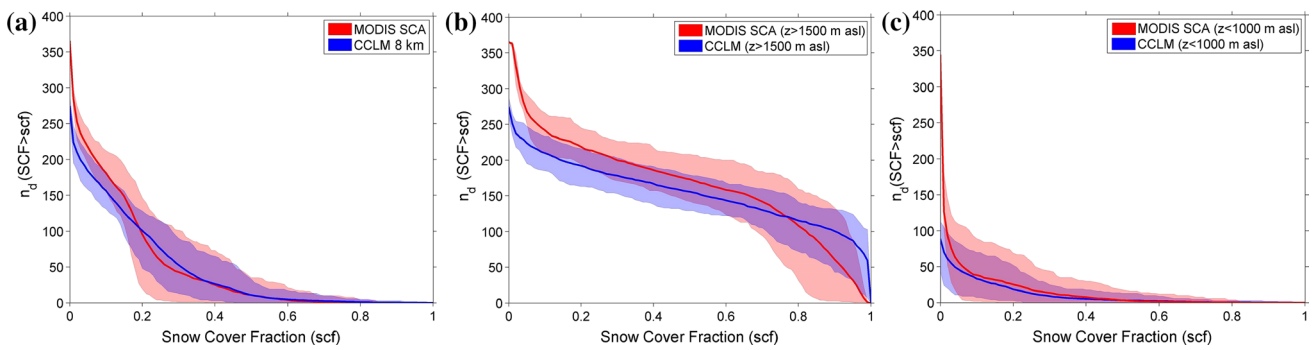
Fig. 10 Comparison between observed (cloud-free MODIS SCA product) and simulated (COSMO-CLM 8 km) average snow cover duration curve for the Po river basin. Panel **a** refers to the entire basin, panel **b** refers to the area above 1500 m asl and panel **c** to that under 1000 m asl. The *shaded area* represents the range between the minimum and maximum values of n_d found in the 9 year sample (2003–2011) for each value of *SCF*
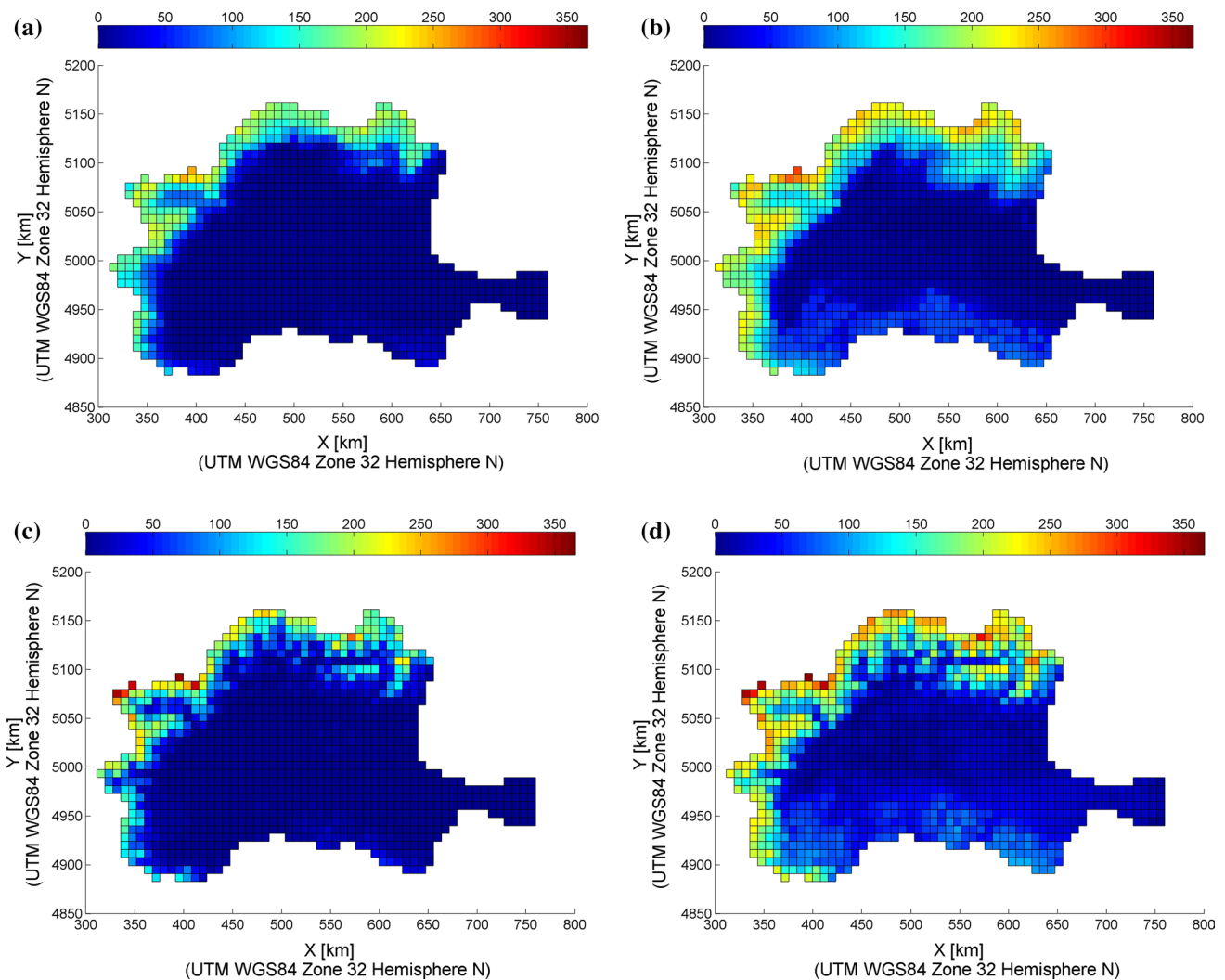

Fig. 11 Comparison between observed (cloud-free MODIS SCA product) and simulated (COSMO-CLM 8 km) snow cover duration maps for the Po river basin. Each cell contains the information on the Snow Cover Days (SCDs). Year 2007 (**a**, **c**) Dec 2006/Feb 2007 average temperature within the basin of about 3 °C and 2010 (**b**, **d**) Dec 2009/Feb 2010 1 °C. Values range from 0 (lowlands) to 365 (glaciers). **a** CCLM 2007, **b** CCLM 2010, **c** MODIS-derived 2007, **d** MODIS-derived 2010

is given. Daily and average weekly values are reported. In spring, the observed snow lines are well reproduced by the model. There is agreement between the growth rate of snow covered altitudes from March to the end of May. The snow lines show differences in the late spring, when the snow extent is too limited to be captured by RCM simulations performed at 8 km resolution. Sudden decreases of the average snow cover elevation reflect occasional extensive snowfall and are properly detected by COSMO-CLM. Considering also the disagreement between the DEMs involved, which have a different source and spatial resolution, COSMO-CLM snowline simulations appear satisfactory for all the years. The comparison between the snowline for the different years (Fig. 9) reveals the capability of COSMO-CLM in simulating the inter-annual changes of snow cover distribution with elevations. For example, it is possible to note the evident differences between snowlines following the mild winter 2006/2007 and the cold winter 2008/2009. In the first case the average elevation of the SCas reaches 2500 m asl before the end of March. In March 2009 the snowline altitude is still lower than 2000 m asl, reaching 2500 m asl about 1 month later. The different behavior is accurately captured by the RCM.

5.1.4 Snow cover duration curves

The snow cover duration curve has been computed for each year, showing that the inter-annual variability of basin-scale snow duration retrieved from MODIS data is well reproduced by the simulation. Since the exceedance frequency of SCF is derived from the time series $SCF(t)$ (Fig. 6), systematic overestimations and underestimations of the snow cover extent reflect also on the snow cover duration. Thus, the snow duration is mostly overestimated for the higher values of SCF, which characterizes the winter months. On the contrary, the duration of the lower snow

covered fractions is underestimated as result of the early depletion of the modeled snow cover. At the basin scale, in all the considered years observed and simulated snow duration curves intercept around the snow cover fraction that is exceeded in about 100 days. Such days are those included in the winter season (December–March), when snow cover extent exceeds 20 % of the domain. These results allow to affirm that snow cover extent and duration are overestimated by COSMO-CLM in winter, while a clear tendency to underestimate is detectable during the spring. As a summary, in the left panel of Fig. 10, we reported the mean snow cover duration curve, evaluated as the average number of days having SCF greater than scf, n_d, where $0 \leq scf \leq 1$. n_d is computed as average of 9 values, belonging to the 9 years. In addition, the shaded regions represent the area between the maximum and minimum values of n_d found within the 9 year sample. It should be pointed that, fixed a certain value of scf, the maximum n_d derived from observation and that obtained from COSMO-CLM could belong to different years. That said, the maximum variability between the 9 curves obtained from COSMO-CLM is similar to that extracted from MODIS SCA. In Fig. 10, the central panel includes the same analysis but limiting the domain to the area that lies above 1500 m asl. Even when only considering the mountainous area, the duration of the lower values of SCF (linked to late winter and spring) is underestimated (be aware that the comparison loses its meaning for the values of SCF close to 0, due to the different spatial resolution of the two datasets). In winter, when the upper part of the domain tends to be entirely snow covered ($SCF \approx 1$), COSMO-CLM overestimates the large-scale snow duration. Averaged over the 9 years, the number of days having this altitude range completely snow covered reaches 100 days in the simulation. On the other side, from the satellite observations we found that $SCF = 85\%$ is exceeded in about 100 days on average. Finally, the right
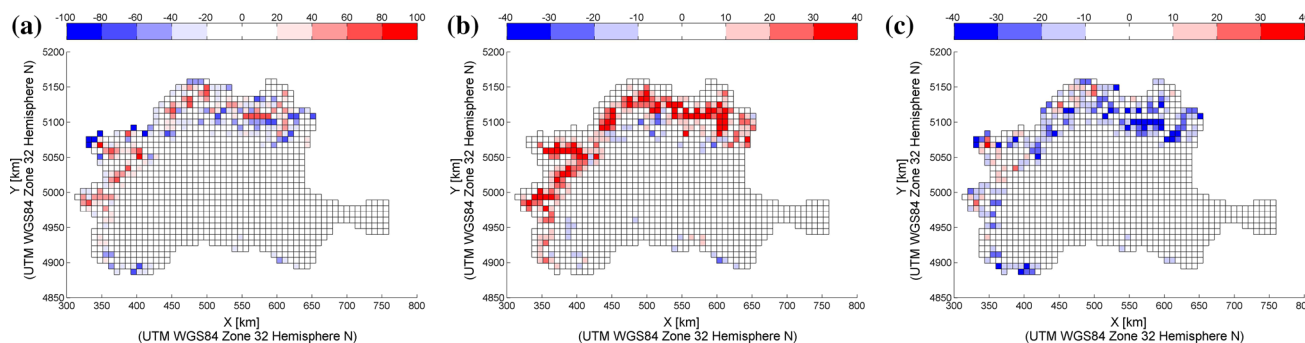

Fig. 12 Maps of average snow cover duration bias (COSMO-CLM–MODIS) computed over the entire year [panel (**a**)], over the period December–January–February [panel (**b**)] and over the period March–April–May [panel (**c**)]. The values reported represent the average bias for the 9 year period. *Blue pixels* indicate underestimation of snow cover duration, while *red* cells indicate overestimations. When only one season in considered, the maximum bias is $+/- 90$ days. On annual basis it can vary from $-365(-366)$ to $+365(+366)$ days of snow cover. **a** Whole year, **b** Winter, **c** Spring

Fig. 13 Observed (cloud-free MODIS SCA product) versus simulated (COSMO-CLM) average monthly Snow Cover Fraction for the Po river basin. The simulations are performed at 8 and 14 km model resolutions. The results refer to the mean values computed over the 9 year period (2003–2011)
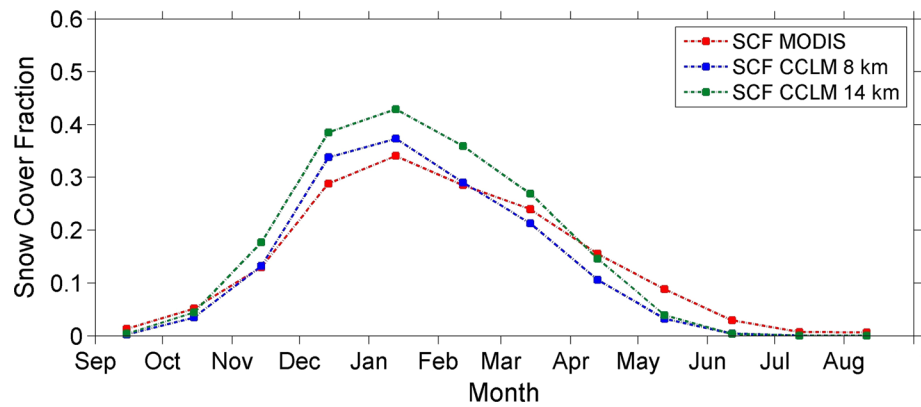
panel of Fig. 10 reports the observed and simulated average snow cover duration curves for the lowest ARC ($z < 1000$ m asl), which contains more than half of the river basin. Here, one can notice that the life of snow cover extent is slightly shorter in COSMO-CLM for all *scf* values.

5.1.5 Snow cover duration maps

We report in Fig. 11 MODIS and COSMO-CLM derived snow duration maps following a mild winter (Dec 2006–Feb 2007, average temperature within the basin of about 3 °C) and a cold winter (Dec 2009–Feb 2010, 1 °C). Values range from 0 to 365 days, since the considered period is the calendar year. Here, the assessment must consider that the observational dataset undergoes firstly a procedure of cloud removal, which preserves the daily resolution of the information, and secondly a resample from the 500 m resolution of the MODIS images to the 8 km resolution of COSMO-CLM grid. Both of these procedures are sources of uncertainty. With respect to this limitation, the coupling of COSMO-CLM and TERRA_ML generates snow cover duration maps able to reproduce the inter-annual variability of the snow cover days. The higher temperatures characterizing the winter months in 2006/2007 impact on snow duration at the annual scale, due to the lower accumulation and the anticipated snowmelt affecting mid elevations. This process is substantially captured by the model. Overall, the spatial pattern of the snow cover duration over the Po river basin is rightly simulated by the COSMO-CLM experiment in all the testing years.

Snow duration maps have the added value of providing a spatially-distributed information on the bias (Fig. 12). This allows to locate those areas most affected by errors. The bias is computed at the pixel scale as difference between simulated and observed Snow Cover Days (SCDs):

$$SCDs_{bias} = SCDs_{sim} - SCDs_{obs} \qquad (4)$$

When assessed at annual scale, it ranges from $-365(-366)$ to $+365(+366)$ days having snow at the ground. Overall,

COSMO-CLM presents a tendency to overestimate snow duration on the Alps [Fig. 12 panel (a)]. Simulated snow cover duration follows the topography properly and in agreement with the maps derived from MODIS data, showing, however, a smoother distribution of values over the altitudes. Under- and over-estimations of snow duration affect especially the transition altitudes, where orographic effects play a key role. The disagreements are basically contained within a range of ±50 days of snow cover. The tendency to overestimate is linked to the overestimation of winter *SCF*, and it is evident in valleys relatively narrow and lengthened such as the Aosta and Adda valleys, drained by Dora Baltea and Adda rivers respectively (see Fig. 1 for the spatial location of these basins). Here, the simulated snow cover durations are more similar to those of the surrounding reliefs, while a stronger altitudinal gradient is found in the resampled observational dataset. Systematic underestimation of the snow cover days characterizes the northeast part of the domain, in Lombardy. What we found at the annual scale is the sum of the winter and spring bias. In particular, the overestimation of the snow cover days in the major Alpine valley is due to the high overestimation of snow duration in winter [Fig. 12 panel (b)]. In spring [March–April–May, Fig. 12 panel (c)], the underestimation of snow cover duration is most evident for the transition elevations. This outcome reflects the anticipated complete snowmelt highlighted by the depletion curves in Fig. 8. A slight tendency to overestimate snow cover duration in spring can be noticed only in the northwest mountain zone, near the highest peaks of the Gran Paradiso and Monte Bianco groups.

5.2 COSMO-CLM 0.0715° versus 0.125°

We investigated whether improvements in modeling the snow cover behavior occur in COSMO-CLM simulations performed at 8 km resolution respect to the 14 km model setup. Enhancements should be ensured by a better representation of the orography, whose effects on climate are
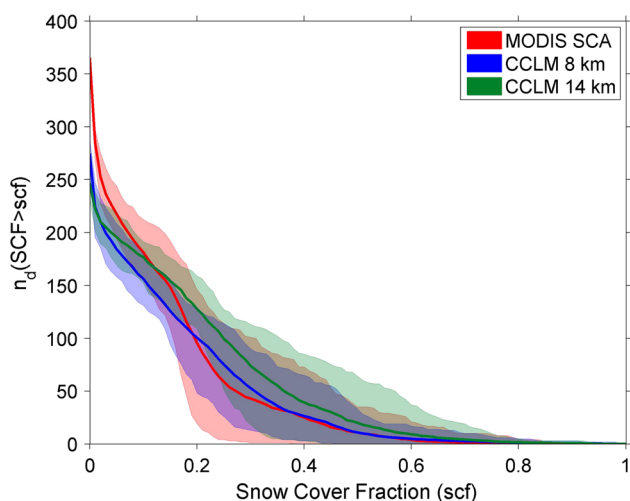
Fig. 14 Observed (cloud-free MODIS SCA product) versus simulated (COSMO-CLM) average snow cover duration curves for the Po river basin. The simulations are performed at 8 and 14 km model resolutions. The *shaded area* represents the range between the minimum and maximum values of n_d found in the 9 year sample for each value of *SCF*

determinant in complex mountain domains (Dutra et al. 2011; Kotlarski et al. 2012; Steger et al. 2013). Montesarchio et al. (2014) showed improvements in climate simulations for the Alps comparing COSMO-CLM simulations run at 8 km resolution with respect to 14 km. Benefits should be reflected even by TERRA_ML variables such as snow cover extent and duration.

Figure 13 shows the temporal evolution of *SCF* reporting the mean monthly values found in the 9 year period. The 14 km experiment substantially overestimates *SCF* in December, January and February. This helps in maintaining higher percentage of spring snow cover extents. However, considering the depletion rate $\frac{dSCF}{dt}$, the 8 km simulation provides a more accurate slope of the depletion curves. Overall, observing the average monthly values over the entire year, 8 km COSMO-CLM provides the best agreement with observations, balancing *SCF* overestimation in winter and underestimation in spring. Table 3 gives a quantitative assessment of this outcome by comparing observed and modeled average weekly values of *SCF* from January to June. The 8 km simulation reduces the *RMSE* over the entire study period. The same statistic, computed using the cloud-reduced maps from the first step of the cloud removal procedure, confirms the better performance of the high-resolution experiment.

The greater capability of the 8 km setup in simulating the relationship between snow cover duration and snow cover fraction at the basin scale can be seen in Fig. 14. The observed average snow cover duration curve is well reproduced by the 8 km experiment. The 14 km setup shows greater overestimations of the snow duration in winter and underestimations in spring. This behavior emerges in all the years of validation.

Overall, these outcomes support the idea that high model resolutions ensure a more realistic representation of the climate in complex mountain domains. The better capability of the 8 km RCM in reproducing the observed atmospheric forcings in the Alpine space is reflected in the spatio-temporal evolution of the snow cover.

6 Discussion and conclusions

The temporal window covered by several remote sensing products already exceeds a decade. Regarding snow cover

Table 3 Values of *NSE* and *RMSE* from the comparison of observed (cloud-free MODIS SCA) and simulated (COSMO-CLM 8 and 14 km setups) average weekly values of *SCF* during the period January–June

Year	COSMO-CLM 0.0715°			COSMO-CLM 0.125°		
	Cloud-free		Step 1	Cloud-free		Step 1
	NSE	RMSE	RMSE	NSE	RMSE	RMSE
2003	0.89	0.04	0.03	0.71	0.05	0.05
2004	0.78	0.06	0.06	0.62	0.08	0.06
2005	0.77	0.06	0.05	0.40	0.09	0.09
2006	0.76	0.07	0.08	0.58	0.09	0.07
2007	0.80	0.03	0.03	0.27	0.05	0.06
2008	0.61	0.06	0.02	0.50	0.06	0.06
2009	0.93	0.05	0.04	0.81	0.09	0.09
2010	0.82	0.07	0.06	0.61	0.10	0.06
2011	0.82	0.05	0.03	0.69	0.05	0.04

Regarding the 14 km experiment, the last column contains the *RMSE* evaluated with respect to cloud-reduced images available after combining Aqua and Terra data. In this case, the comparison is limited to those days having <5 % cloud cover after being processed by Step 1 of the cloud removal procedure (Da Ronco and De Michele 2014)

Fig. 15 Comparison between observed (EURO4M/EOBS/ MODIS SCA) and simulated (COSMO-CLM 8 km) daily precipitation (*top panel*), temperature (*median panel*) and snow cover fraction (*lower panel*) for 2004. The values of temperature and precipitation are averaged over the Alpine region (altitude above 1000 m asl)
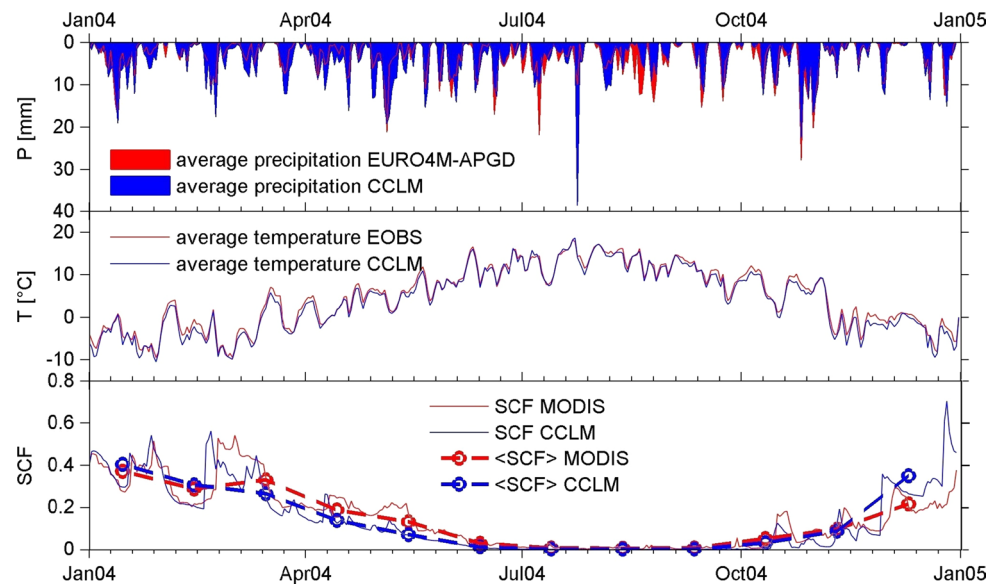
dynamics, in perspective the tools based on EO (Earth Observation) will acquire more importance for validating climate models, supporting gridded datasets based on ground measurements. In fact, the latter require spatialization techniques for evaluating point values in space and they need a dense network of ground stations.

This paper presents a methodology to assess snow cover simulations by RCMs using high-resolution EO maps. We account both for snow cover duration, distribution and extension performing basin-scale and cell-scale evaluations. Some analyses are performed at the year-scale, while others investigate spring and winter independently. The detection of the spatial and seasonal behavior of the bias is definitely important as it can direct the investigation of the sources of RCM inaccuracy.

The methodology presented here can be applied to different RCMs using as reference binary snow cover maps from EO. As an application, we have assessed two snow cover simulations driven by the Regional Climate Model COSMO-CLM. The RCM is coupled with the multi-layer soil and vegetation model TERRA_ML. Remote sensing data from MODIS are used as observational dataset after a pre-processing of the binary products in MOD10A1 and MYD10A1 (2003–2011). The variables under examination are snow cover duration, distribution and snow cover extent. Referring to these outputs, COSMO-CLM is capable to reproduce their inter-seasonal and inter-annual variability with a good level of accuracy when run at 8 km resolution. Even the timings of the snow processes are rightly captured, as well as snow cover duration at the basin-scale. However, systematic bias emerges both in winter and spring while increasing the temporal scale of analysis. In particular, the results show that the depletion rate during the melting period is overestimated leading to early complete snowmelt for all altitude bands and to the underestimation of snow cover duration. This would adversely affect the climate simulations in the atmospheric layers, given that snow cover changes significantly the surface albedo and the surface temperature. Since topographic effects impact on snow cover dynamics, we studied whether a higher spatial resolution of the model provides advantages in simulating variables such as snow cover extent and duration. The results indicate that snow cover extent and duration approach those observed in winter increasing the model resolution (from 14 to 8 km). Hence, a higher resolution is beneficial to simulate the accumulation processes of the snow cover on the Alps. This outcome agrees with what found by Montesarchio et al. (2014) for the same case study, comparing 8 and 14 km simulated temperatures with the observations. On the contrary, determinant advantages do not emerge for modeling spring snow cover extent, even though the slope of the depletion curve is more similar to the observed one when the 8 km setup is used. With respect to snow cover, the causes of disagreement with observations shown by all model setups could descend from the parameterization of the snow processes in TERRA_ML or from biases in the forcing inputs as temperature or precipitation. In Fig. 15 we link the temporal trend of the snow cover extent to temperature and precipitation bias in the COSMO-CLM 8 km run. Simulated Alpine temperature is compared to the average values from the E-OBS gridded dataset (Van der Schrier et al. 2013) while precipitation is compared to that derived from the EURO4M dataset (Isotta et al. 2014). The plot refers to the period January–December 2004, but a similar behaviour characterized the other years. Figure 15 indicates that the overestimation of winter snow cover extent can be reasonably linked to temperature underestimation. On the one hand, underestimation of regional temperature implies

a wider domain subjected to conditions suitable to snow-falls. On the other hand, lower temperatures make it difficult to have important melting during winter. As response, larger areas with snow on the ground contribute in maintaining low temperatures due to the high snow albedo. In addition, average precipitation is slightly overestimated during the winter months, thus increasing snow amounts accumulating on the ground. Regarding the underestimation of snow cover extent and duration in spring, the reasons for COSMO-CLM inaccuracy might be sought in TERRA_ML snow module where snowmelt is modeled. In fact, Bucchignani et al. (2016) showed that the same model setup underestimates spring temperatures, which in itself should protect snow cover from early melting. Further investigations will be directed to this issue.

Our study fits within a line of contributions dealing with the reliability of RCM snow cover simulations (Räisänen and Eklund 2012; Kotlarski et al. 2012; Klehmet et al. 2013; Steger et al. 2013). First of all, it suggests some innovative directions for comparing RCM outputs with observations, introducing EO data and some derived products. The strategy presented here can work in parallel to other validation methods that make use of ground measurements of snow depth or SWE. For example, the recent study by Steger et al. (2013) presents a detailed evaluation of different RCMs forced by the ERA-40 re-analysis (Uppala et al. 2005) in Switzerland. For comparing model results and observations at 110 stations, they firstly converted the measured snow depths to SWE. Secondly, they mapped the result on the ensemble mean orography using non-linear SWE lapse rates as suggested in Foppa et al. (2007). Then, they carried out the validation excluding those cells having altitude >2100 m asl, since only one station above this height had long-term data, and the assessment period was restricted to December-April for all the measuring points. The most of the zones excluded from the validation fall right on the border with the Italian Alps. Nonetheless, in the climate projection part the winter season encompassed the period November–April and the elevation bands considered exceeded 2500 m asl, involving regions and periods that were not explored in the validation due to the lack of data. The unavoidable gaps left by a dataset that cannot be collected with continuous and uniform distribution over wide and complex domains can be overcome using satellite observations. The availability of EO data does not depend on altitude or season, especially when the source products are processed to reduce cloud obstruction [note that in the Alps the latter affects mostly winter months and altitude over 1000 m asl as shown in Da Ronco and De Michele (2014)]. Focusing specifically on COSMO-CLM, in the work by Kotlarski et al. (2012) the snow field of the RCM is considered for proposing a trend of Alpine snow cover dynamics, as consequence of changing atmospheric forcings. However, there is no evaluation

of the reliability of these snow cover simulations. Klehmet et al. (2013) used the ESA GlobSnow products to compare COSMO-CLM forced by NCEP-R1 to global reanalyses for the period 1987–2010. They demonstrated the added value of COSMO-CLM in representing a more realistic spatio-temporal evolution of SWE if compared to that provided by NCEP-R1 itself. However, the outcomes refer to Siberia, the resolution of the RCM is about 50 km and the model setup includes an improved version of the COSMO-CLM snow module included in TERRA_ML. The topographic and climatic differences between the regions make the results by Klehmet et al. (2013) non-transferable to the Alpine space.

Discussing the performances of COSMO-CLM in the context of other regional climate simulations, we can compare our results to those reported in Steger et al. (2013) for different RCMs and for their ensemble mean. The spatial domains of analysis are complementary as Steger et al. (2013) investigated the northern valleys of the Alps, in Switzerland, while our focus is on the southern region facing Italy. A direct and exhaustive comparison is not possible since the variables investigated in our study do not include snow density and snow water equivalent and the spatial resolutions are different. Both studies conclude that the ERA-driven RCMs are able to reproduce the basic spatial pattern of snow cover and the inter-seasonal and inter-annual variability of its response. In the assessment of COSMO-CLM performance, we consider snow cover duration as key variable. Even Steger et al. (2013) provide information on snow cover duration bias but only for elevations lower than 1000 m asl and for the period December–April. Specifically, for the lowest ARC ($z < 1000$ m asl) they highlight the underestimation of the life of the snow cover with respect to observations, affecting all the tested RCMs. On annual basis, the 8 km COSMO-CLM simulation ensures good agreement with observed snow cover duration for all altitude bands. A spatial pattern of the bias exists, having greater overestimations of snow duration in the western Alps and a slight propensity to overestimate in the central and east slopes. Even if the bias does not reveal a uniform tendency to underestimate snow duration within the basin, for altitudes lower than 1000 m asl the snow cover duration curves derived from both 8 and 14 km COSMO-CLM experiments strengthen the conclusion proposed by Steger et al. (2013). Indeed, the duration of the simulated snow cover extent is slightly underrated by both setups in the lowest ARC. However, what we found at the year scale is the sum of a clear tendency to overestimate snow duration in winter and to underestimate it in spring. Focusing on spring, mid and low altitudes are heavily affected by underestimation all over the Po river basin. Thus, a clear underestimation of snow duration exists only in the melting months in our experiment. To get other points of comparison between our work and Steger et al. (2013), we could

hypothesize that SWE overestimates imply larger SCA and longer snow duration while SWE underestimates suggest lower snow coverages and earlier disappearance of snow in spring. These are all variables governed by the same key meteorological forcings: the simulation of colder and rainier winters compared to the observations conducts to the overestimation of SWE but also to a longer duration of coverage and, reasonably, excessive extension. Steger et al. (2013) indicate noticeable underestimations of mean winter SWE (period December–April) in the majority of the models for the region below 1000 m asl and, in some cases, between 1000 and 1500 m asl, with lower bias for the second ARC. As already mentioned, in the COSMO-CLM experiments these altitude range classes are subjected to greater errors respect to the highest ARC. The bias affects both SCDs and *SCF* but its sign depends on the season and on the spatial location. Thus, our results do not fully confirm what stated in Steger et al. (2013). Then, Steger et al. (2013) report a slight tendency to overestimate mean winter SWE in the highest altitude range where the validation was performed (1500–2100 m asl), affecting the majority of the models. Focusing on the accumulation months, we found overestimation of the snow cover extent and duration in the mountain part of the domain, in agreement with the outcome by Steger et al. (2013). The common conclusion is that some bias in the atmospheric forcings may exist determining the overestimation of snow inputs in winter for the Alpine space. The first suspicion falls necessarily on underestimation of temperature, but both studies indicate also the pronounced overestimation of precipitation in mountain as a possible culprit. This point is relevant since the observational snow data used for the comparison in our manuscript and in that by Steger et al. (2013) are manipulated for being comparable with RCMs snow cover outputs. Despite this, they conducted to similar conclusions.

Thanks to the snow cover duration maps, a novel aspect that emerged from our investigation is that, taking narrow and lengthened valley such as the Dora Baltea and the Adda river basins, the variability of snow cover days with altitude is less pronounced than that obtained from MODIS. There, altitude varies strongly over short distances at both sides of the valleys and the model, even if it is run at really high resolution (8 km), does not capture the pronounced variation of the snow cover days between neighboring cells. As result, in these valleys the snow cover duration is clearly overestimated in winter. This outcome can be seen as response of the smoother topography used in COSMO-CLM compared to the resampling of the 500 m DEM. The 8 km model setup allows to catch this behavior that would be difficult to uncover adopting resolutions in the order of 20 km. In fact, where topography changes suddenly over short plain distances, a 20 km square cell can cover entirely the area between one side of the valley and the other.

The conclusions presented here about the bias dependence on the RCM spatial resolution could be tested by incoming investigations which consider 2.2 km snow cover outputs from COSMO-CLM.

References

Agrawala S et al (2007) Climate change in the European Alps: adapting winter tourism and natural hazards management, vol 2. OECD publishing

Barnett T, Dümenil L, Schlese U, Roeckner E, Latif M (1989) The effect of Eurasian snow cover on regional and global climate variations. J Atmos Sci 46(5):661–686

Barnett TP, Adam JC, Lettenmaier DP (2005) Potential impacts of a warming climate on water availability in snow-dominated regions. Nature 438(7066):303–309

Bavay M, Lehning M, Jonas T, Löwe H (2009) Simulations of future snow cover and discharge in Alpine headwater catchments. Hydrol Process 23(1):95–108

Bavera D, De Michele C (2009) Snow water equivalent estimation in the Mallero basin using snow gauge data and MODIS images and fieldwork validation. Hydrol Process 23(14):1961–1972. doi:10.1002/hyp.7328

Beniston M (2003) Climatic change in mountain regions: a review of possible impacts. In: Climate variability and change in high elevation regions: past, present and future. Springer, Dordrecht, pp 5–31. doi:10.1007/978-94-015-1252-7_2

Beniston M (2005) Mountain climates and climatic change: an overview of processes focusing on the European Alps. Pure Appl Geophys 162(8–9):1587–1606. doi:10.1007/s00024-005-2684-9

Beniston M, Rebetez M (1996) Regional behavior of minimum temperatures in Switzerland for the period 1979–1993. Theoret Appl Climatol 53(4):231–243. doi:10.1007/BF00871739

Beniston M, Keller F, Goyette S (2003) Snow pack in the Swiss Alps under changing climatic conditions: an empirical approach for climate impacts studies. Theoret Appl Climatol 74(1–2):19–31

Beniston M, Keller F, Koffi B, Goyette S (2003) Estimates of snow accumulation and volume in the Swiss Alps under changing climatic conditions. Theoret Appl Climatol 76(3–4):125–140

Brander D, Seidel K, Huggel C, Zurflueh M (2000) Snow cover duration maps in alpine regions from remote sensing data. In: Proceedings of EARSeL-SIG-Workshop Land Ice and Snow, vol 80, Dresden

Brown RD, Mote PW (2009) The response of northern hemisphere snow cover to a changing climate. J Clim 22(8):2124–2145. doi:10.1175/2008JCLI2665.1

Brutel-Vuilmet C, Ménégoz M, Krinner G (2013) An analysis of present and future seasonal Northern Hemisphere land snow cover simulated by CMIP5 coupled climate models. Cryosphere 7(1):67–80. doi:10.5194/tc-7-67-2013

Bucchignani E, Sanna A, Gualdi S, Castellari S, Schiano P (2013) Simulation of the climate of the XX century in the Alpine space. Nat Hazards 67(3):981–990. doi:10.1007/s11069-011-9883-8

Bucchignani E, Montesarchio M, Zollo AL, Mercogliano P (2016) High resolution climate simulations with COSMO-CLM over Italy: performance evaluation and climate projections for

the 21st century. Int J Climatol 36(2):735–756. doi:10.1002/joc.4379

Chai T, Draxler RR (2014) Root mean square error (RMSE) or mean absolute error (MAE)?—Arguments against avoiding RMSE in the literature. Geosci Model Dev 7(3):1247–1250. doi:10.5194/gmd-7-1247-2014

Chang ATC, Gloersen P, Schmugge T, Wilheit TT, Zwally HJ (1976) Microwave emission from snow and glacier ice. J Glacio 16:23–39

Chang N, Hong Y (2012) Multiscale hydrologic remote sensing: perspectives and applications. CRC Press, Taylor & Francis Group, Boca Raton

Christensen J, Christensen O (2007) A summary of the PRUDENCE model projections of changes in European climate by the end of this century. Clim Change 81(1):7–30. doi:10.1007/s10584-006-9210-7

Christensen NS, Wood AW, Voisin N, Lettenmaier DP, Palmer RN (2004) The effects of climate change on the hydrology and water resources of the Colorado river basin. Clim Change 62(1–3):337–363

Clifford D (2010) Global estimates of snow water equivalent from passive microwave instruments: history, challenges and future developments. Int J Remote Sens 31(14):3707–3726. doi:10.1080/01431161.2010.483482

Cohen J, Rind D (1991) The effect of snow cover on the climate. J Clim 4(7):689–706

Comola F, Schaefli B, Da Ronco P, Botter G, Bavay M, Rinaldo A, Lehning M (2015) Scale-dependent effects of solar radiation patterns on the snow-dominated hydrologic response. Geophys Res Lett 42(10):3895–3902. doi:10.1002/2015GL064075

Da Ronco P, De Michele C (2014) Cloud obstruction and snow cover in Alpine areas from MODIS products. Hydrol Earth Syst Sci 18(11):4579–4600. doi:10.5194/hess-18-4579-2014

Davin E, Stöckli R, Jaeger E, Levis S, Seneviratne S (2011) COSMO-CLM²: a new version of the COSMO-CLM model coupled to the Community Land Model. Clim Dyn 37(9–10):1889–1907. doi:10.1007/s00382-011-1019-z

Dee D, Uppala S, Simmons A, Berrisford P, Poli P, Kobayashi S, Andrae U, Balmaseda M, Balsamo G, Bauer P et al (2011) The ERA-Interim reanalysis: configuration and performance of the data assimilation system. Q J R Meteorol Soc 137(656):553–597

Dietz AJ, Kuenzer C, Gessner U, Dech S (2012) Remote sensing of snow-a review of available methods. Int J Remote Sens 33(13):4094–4134

Doms G, Förstner J, Heise E, Herzog H, Mironov D, Raschendorfer M, Reinhardt T, Ritter B, Schrodin R, Schulz JP, Vogel G (2011) A description of the nonhydrostatic regional COSMO model. Part II: Physical parameterization. Deutscher Wetterdienst

Dozier J (1989) Spectral signature of alpine snow cover from the Landsat Thematic Mapper. Remote Sens Environ 28(0):9–22. doi:10.1016/0034-4257(89)90101-6

Dutra E, Kotlarski S, Viterbo P, Balsamo G, Miranda PMA, Schär C, Bissolli P, Jonas T (2011) Snow cover sensitivity to horizontal resolution, parameterizations, and atmospheric forcing in a land surface model. J Geophys Res Atmos 116(D21). doi:10.1029/2011JD006061

Elder K, Rosenthal W, Davis RE (1998) Estimating the spatial distribution of snow water equivalence in a montane watershed. Hydrol Process 12(10–11):1793–1808. doi:10.1002/(SICI)1099-1085(199808/09)12:10/11<1793::AID-HYP695>3.0.CO;2-K

Elsasser H, Bürki R et al (2002) Climate change as a threat to tourism in the Alps. Clim Res 20(3):253–257

Erschbamer B, Kiebacher T, Mallaun M, Unterluggauer P (2009) Short-term signals of climate change along an altitudinal gradient in the South Alps. Plant Ecol 202(1):79–89

Feldmann H, Schädler G, Panitz HJ, Kottmeier C (2013) Near future changes of extreme precipitation over complex terrain in Central Europe derived from high resolution RCM ensemble simulations. Int J Climatol 33(8):1964–1977. doi:10.1002/joc.3564

Fletcher CG, Kushner PJ, Hall A, Qu X (2009) Circulation responses to snow albedo feedback in climate change. Geophys Res Lett 36(9):L09702. doi:10.1029/2009GL038011

Foppa N, Seiz G (2012) Inter-annual variations of snow days over Switzerland from 2000–2010 derived from MODIS satellite data. Cryosphere 6(2):331–342. doi:10.5194/tc-6-331-2012

Foppa N, Stoffel A, Meister R (2007) Synergy of in situ and space borne observation for snow depth mapping in the Swiss Alps. Int J Appl Earth Obs Geoinf 9(3):294–310. doi:10.1016/j.jag.2006.10.001

Foster JL, Sun C, Walker JP, Kelly R, Chang A, Dong J, Powell H (2005) Quantifying the uncertainty in passive microwave snow water equivalent observations. Remote Sens Environ 94(2):187–203. doi:10.1016/j.rse.2004.09.012

Fowler HJ, Blenkinsop S, Tebaldi C (2007) Linking climate change modelling to impacts studies: recent advances in downscaling techniques for hydrological modelling. Int J Climatol 27(12):1547–1578. doi:10.1002/joc.1556

Frei A, Tedesco M, Lee S, Foster J, Hall DK, Kelly R, Robinson DA (2012) A review of global satellite-derived snow products. Adv Space Res 50(8):1007–1029

Frei C, Christensen JH, Déqué M, Jacob D, Jones RG, Vidale PL (2003) Daily precipitation statistics in regional climate models: evaluation and intercomparison for the European Alps. J Geophys Res Atmos 108(D3). doi:10.1029/2002JD002287

Gafurov A, Bárdossy A (2009) Cloud removal methodology from MODIS snow cover product. Hydrol Earth Syst Sci 13(7):1361–1373. 10.5194/hess-13-1361-2009

Gao Y, Xie H, Yao T (2011) Developing snow cover parameters maps from MODIS, AMSR-E, and blended snow products. Photogramm Eng Remote Sens 77(4):351–361

Gascoin S, Hagolle O, Huc M, Jarlan L, Dejoux JF, Szczypta C, Marti R, Sánchez R (2015) A snow cover climatology for the Pyrenees from MODIS snow products. Hydrol Earth Syst Sci 19(5):2337–2351. doi:10.5194/hess-19-2337-2015

Gesell G (1989) An algorithm for snow and ice detection using AVHRR data an extension to the APOLLO software package. Int J Remote Sens 10(4–5):897–905

Giorgi F, Lionello P (2008) Climate change projections for the Mediterranean region. Global Planet Change 63(2):90–104

Giorgi F, Hurrell JW, Marinucci MR, Beniston M (1997) Elevation dependency of the surface climate change signal: a model study. J Clim 10(2):288–296

Giorgi F, Christensen J, Hulme M, von Storch H, Whetton P, Jones R, Mearns L, Fu C, Arritt R, Bates B, Benestad R, Boer G, Buishand A, Castro M, Chen D, Cramer W, Crane R, Crossly J, Dehn M, Dethloff K, Dippner J, Emori S, Francisco R, Fyfe J, Gerstengarbe F, Gutowski W, Gyalistras D, Hanssen-Bauer I, Hantel M, Hassell D, Heimann D, Jack C, Jacobeit J, Kato H, Katz R, Kauker F, Knutson T, Lal M, Landsea C, Laprise R, Leung L, Lynch A, May W, McGregor J, Miller N, Murphy J, Ribalaygua J, Rinke A, Rummukainen M, Semazzi F, Walsh K, Werner P, Widmann M, Wilby R, Wild M, Xue Y (2001) Regional Climate Information- Evaluation and Projections, Climate Change 2001: The Scientific Basis. In: [Houghton JT et al (eds)] Contribution of Working Group to the Third Assessment Report of the Intergouvernmental Panel on Climate Change. Cambridge University Press, Cambridge, New York, p 881

Giorgi F, Jones C, Asrar GR et al (2009) Addressing climate information needs at the regional level: the CORDEX framework. World meteorological organization (WMO). Bulletin 58(3):175

Gobiet A, Kotlarski S, Beniston M, Heinrich G, Rajczak J, Stoffel M (2013) 21st century climate change in the European Alps—A review. Sci Total Environ 493:1138–1151. doi:10.1016/j.scitotenv.2013.07.050

Grasselt R, Schüttemeyer D, Warrach-Sagi K, Ament F, Simmer C (2008) Validation of TERRA-ML with discharge measurements. Meteorol Z 17(6):763–773. doi:10.1127/0941-2948/2008/0334

Haeberli W, Beniston M (1998) Climate change and its impacts on glaciers and permafrost in the Alps. Ambio 27(4):258–265

Hall A (2004) The role of surface albedo feedback in climate. J Clim 17(7):1550–1568. doi:10.1175/1520-0442(2004)017<1550:TROSAF>2.0.CO;2

Hall DK, Riggs GA (2007) Accuracy assessment of the MODIS snow products. Hydrol Process 21(12):1534–1547

Hall DK, Riggs GA, Salomonson VV (1995) Development of methods for mapping global snow cover using moderate resolution imaging spectroradiometer data. Remote Sens Environ 54(2):127–140

Hall DK, Riggs GA, Salomonson VV, Barton J, Casey K, Chien J, DiGirolamo N, Klein A, Powell H, Tait A (2001) Algorithm theoretical basis document (ATBD) for the MODIS snow and sea ice-mapping algorithms. NASA GSFC

Hall DK, Riggs GA, Salomonson VV, DiGirolamo NE, Bayr KJ (2002) MODIS snow-cover products. Remote Sens Environ 83(1):181–194

Hall DK, Riggs GA, Foster JL, Kumar SV (2010) Development and evaluation of a cloud-gap-filled MODIS daily snow-cover product. Remote Sens Environ 114(3):496–503. doi:10.1016/j.rse.2009.10.007

Hantel M, Hirtl-Wielke LM (2007) Sensitivity of Alpine snow cover to European temperature. Int J Climatol 27(10):1265–1275

Hantel M, Maurer C (2011) The median winter snowline in the Alps. Meteorol Z 20(3):267–276. doi:10.1127/0941-2948/2011/0495

Hantel M, Maurer C, Mayer D (2012) The snowline climate of the Alps 1961–2010. Theoret Appl Climatol 110(4):517–537. doi:10.1007/s00704-012-0688-9

Haslinger K, Anders I, Hofstätter M (2013) Regional climate modelling over complex terrain: an evaluation study of COSMO-CLM hindcast model runs for the Greater Alpine Region. Clim Dyn 40(1–2):511–529. doi:10.1007/s00382-012-1452-7

Hüsler F, Jonas T, Riffler M, Musial J, Wunderle S (2014) A satellite-based snow cover climatology (1985–2011) for the European Alps derived from AVHRR data. Cryosphere 8(1):73–90

Im ES, Coppola E, Giorgi F, Bi X (2010) Local effects of climate change over the Alpine region: a study with a high resolution regional climate model with a surrogate climate change scenario. Geophys Res Lett 37(5). doi:10.1029/2009GL041801,

Isotta FA, Frei C, Weilguni V, Perčec Tadić M, Lassègues P, Rudolf B, Pavan V, Cacciamani C, Antolini G, Ratto SM, Munari M, Micheletti S, Bonati V, Lussana C, Ronchi C, Panettieri E, Marigo G, Vertačnik G (2014) The climate of daily precipitation in the Alps: development and analysis of a high-resolution grid dataset from pan-Alpine rain-gauge data. Int J Climatol 34(5):1657–1675. doi:10.1002/joc.3794

Jacob D, Petersen J, Eggert B, Alias A, Christensen O, Bouwer L, Braun A, Colette A, Déqué M, Georgievski G, Georgopoulou E, Gobiet A, Menut L, Nikulin G, Haensler A, Hempelmann N, Jones C, Keuler K, Kovats S, Kröner N, Kotlarski S, Kriegsmann A, Martin E, van Meijgaard E, Moseley C, Pfeifer S, Preuschmann S, Radermacher C, Radtke K, Rechid D, Rounsevell M, Samuelsson P, Somot S, Soussana JF, Teichmann C, Valentini R, Vautard R, Weber B, Yiou P (2014) EURO-CORDEX: new high-resolution climate change projections for European impact research. Reg Environ Change 14(2):563–578. doi:10.1007/s10113-013-0499-2

Jonas T, Rixen C, Sturm M, Stoeckli V (2008) How alpine plant growth is linked to snow cover and climate variability. J Geophys Res Biogeosci 113(G3):G03013. doi:10.1029/2007JG000680

Keller F, Goyette S, Beniston M (2005) Sensitivity analysis of snow cover to climate change scenarios and their impact on plant habitats in alpine terrain. Clim Change 72(3):299–319

Klehmet K, Geyer B, Rockel B (2013) A regional climate model hindcast for Siberia: analysis of snow water equivalent. Cryosphere 7(4):1017–1034

Klein AG, Stroeve J (2002) Development and validation of a snow albedo algorithm for the MODIS instrument. Ann Glaciol 34(1):45–52

Klein AG, Hall DK, Riggs GA (1998) Improving snow cover mapping in forests through the use of a canopy reflectance model. Hydrol Process 12(10–11):1723–1744. doi:10.1002/(SICI)1099-1085(199808/09)12:10/11<1723::AID-HYP691>3.0.CO;2-2

Koenig U, Abegg B (1997) Impacts of climate change on winter tourism in the Swiss Alps. J Sustain Tour 5(1):46–58

Kotlarski S, Bosshard T, Lüthi D, Pall P, Schär C (2012) Elevation gradients of European climate change in the Regional Climate Model COSMO-CLM. Clim Change 112(2):189–215. doi:10.1007/s10584-011-0195-5

Kotlarski S, Keuler K, Christensen OB, Colette A, Déqué M, Gobiet A, Goergen K, Jacob D, Lüthi D, van Meijgaard E, Nikulin G, Schär C, Teichmann C, Vautard R, Warrach-Sagi K, Wulfmeyer V (2014) Regional climate modeling on European scales: a joint standard evaluation of the EURO-CORDEX RCM ensemble. Geosci Model Dev Discuss 7(4):1297–13333. doi:10.5194/gmd-7-1297-2014

Krause P, Boyle DP, Bäse F (2005) Comparison of different efficiency criteria for hydrological model assessment. Adv Geosci 5:89–97. doi:10.5194/adgeo-5-89-2005

Kunstmann H, Stadler C (2005) High resolution distributed atmospheric-hydrological modelling for Alpine catchments. J Hydrol 314(1–4):105–124. doi:10.1016/j.jhydrol.2005.03.033

Laternser M, Schneebeli M (2003) Long-term snow climate trends of the Swiss Alps (1931–99). Int J Climatol 23(7):733–750. doi:10.1002/joc.912

Lee S, Klein AG, Over TM (2005) A comparison of MODIS and NOHRSC snow-cover products for simulating streamflow using the Snowmelt Runoff Model. Hydrol Process 19(15):2951–2972. doi:10.1002/hyp.5810

López-Moreno JI, Goyette S, Beniston M (2008) Climate change prediction over complex areas: spatial variability of uncertainties and predictions over the Pyrenees from a set of regional climate models. Int J Climatol 28(11):1535–1550. doi:10.1002/joc.1645

Magnusson J, Jonas T, Lopez-Moreno I, Lehning M (2010) Snow cover response to climate change in a high alpine and haif-glacierized basin in Switzerland. Hydrol Res 41(3–4):230–240. doi:10.2166/nh.2010.115

Martin E, Etchevers P (2005) Impact of climatic changes on snow cover and snow hydrology in the French Alps. In: Huber UM, Bugmann HKM, Reasoner MA (eds) Global change and mountain regions: An overview of current knowledge, Part II. Advances in global change research, vol 23. Springer, Netherlands, pp 235–242. doi:10.1007/140203508X24

Meehl GA, Covey C, Taylor KE, Delworth T, Stouffer RJ, Latif M, McAvaney B, Mitchell JF (2007) The WCRP CMIP3 multi-model dataset: a new era in climate change research. Bull Am Meteorol Soc 88(9):1383–1394

Middelkoop H, Daamen K, Gellens D, Grabs W, Kwadijk JC, Lang H, Parmet BW, Schädler B, Schulla J, Wilke K (2001) Impact of climate change on hydrological regimes and water resources management in the Rhine basin. Clim Change 49(1–2):105–128

Montesarchio M, Zollo AL, Bucchignani E, Mercogliano P, Castellari S (2014) Performance evaluation of high-resolution regional climate simulations in the Alpine space and analysis of extreme events. J Geophys Res Atmos 119(6):3222–3237. doi:10.1002/2013JD021105

Nash J, Sutcliffe J (1970) River flow forecasting through conceptual models part I—A discussion of principles. J Hydrol 10(3):282–290. doi:10.1016/0022-1694(70)90255-6,

Parajka J, Blöschl G (2006) Validation of MODIS snow cover images over Austria. Hydrol Earth Syst Sci 10(5):679–689. doi:10.5194/hess-10-679-2006

Parajka J, Blöschl G (2008a) Spatio-temporal combination of MODIS images – potential for snow cover mapping. Water Resour Res 44(3). doi:10.1029/2007WR006204

Parajka J, Blöschl G (2008b) The value of MODIS snow cover data in validating and calibrating conceptual hydrologic models. J Hydrol 358(3–4):240–258. doi:10.1016/j.jhydrol.2008.06.006

Parajka J, Pepe M, Rampini A, Rossi S, Blöschl G (2010) A regional snow-line method for estimating snow cover from MODIS during cloud cover. J Hydrol 381(3–4):203–212. doi:10.1016/j.jhydrol.2009.11.042

Paudel KP, Andersen P (2011) Monitoring snow cover variability in an agropastoral area in the Trans Himalayan region of Nepal using MODIS data with improved cloud removal methodology. Remote Sens Environ 115(5):1234–1246

Pauli H, Gottfried M, Grabherr G (1996) Effects of climate change on mountain ecosystems—upward shifting of alpine plants. World Resour Rev 8(3):382–390

Payne JT, Wood AW, Hamlet AF, Palmer RN, Lettenmaier DP (2004) Mitigating the effects of climate change on the water resources of the Columbia river basin. Clim Change 62(1–3):233–256

Pepe M, Brivio P, Rampini A, Nodari FR, Boschetti M (2005) Snow cover monitoring in Alpine regions using ENVISAT optical data. Int J Remote Sens 26(21):4661–4667

Räisänen J (2008) Warmer climate: less or more snow? Clim Dyn 30(2–3):307–319. doi:10.1007/s00382-007-0289-y

Räisänen J, Eklund J (2012) 21st century changes in snow climate in northern Europe: a high-resolution view from ENSEMBLES regional climate models. Clim Dyn 38(11–12):2575–2591. doi:10.1007/s00382-011-1076-3

Ramsay BH (1998) The interactive multisensor snow and ice mapping system. Hydrol Process 12(10):1537–1546

Rango A, Chang A, Foster J (1979) The utilization of spaceborne microwave radiometers for monitoring snowpack properties. Nord Hydrol 10(1):25–40

Rango A, Gomez-Landesa E, Bleiweiss M, Havstad K, Tanksley K (2003) Improved satellite snow mapping, snowmelt runoff forecasting, and climate change simulations in the upper Rio Grande basin. World Resour Rev 15:25–41

Riggs G, Hall DK, Salomonson VV (2006) MODIS snow products user guide to collection 5. http://modis-snow-ice.gsfc.nasa.gov

Rittger K, Painter TH, Dozier J (2013) Assessment of methods for mapping snow cover from MODIS. Adv Water Resour 51:367–380

Rockel B, Will A, Hense A (2008) The regional climate model COSMO-CLM (CCLM). Meteorol Z 17(4):347–348

Rodell M, Houser P (2004) Updating a land surface model with MODIS-derived snow cover. J Hydrometeorol 5(6):1064–1075

Salomonson V, Appel I (2004) Estimating fractional snow cover from MODIS using the normalized difference snow index. Remote Sens Environ 89(3):351–360

Salomonson VV, Appel I (2006) Development of the Aqua MODIS NDSI fractional snow cover algorithm and validation results. Geosci Remote Sens IEEE Trans 44(7):1747–1756

Schaefli B, Hingray B, Musy A et al (2007) Climate change and hydropower production in the Swiss Alps: quantification of potential impacts and related modelling uncertainties. Hydrol Earth Syst Sci Dis 11(3):1191–1205

Schaper J, Martinec J, Seidel K (1999) Distributed mapping of snow and glaciers for improved runoff modelling. Hydrol Process 13(12–13):2023–2031. doi:10.1002/(SICI)1099-1085(199909)13:12/13<2023::AID-HYP877>3.0.CO;2-A

Scherrer SC, Appenzeller C, Laternser M (2004) Trends in Swiss Alpine snow days: the role of local- and large-scale climate variability. Geophys Res Lett 31(13). doi:10.1029/2004GL020255,

Van der Schrier G, van den Besselaar EJM, Klein Tank AMG, Verver G (2013) Monitoring European average temperature based on the E-OBS gridded data set. J Geophys Res Atmos 118(11):5120–5135. doi:10.1002/jgrd.50444

Scott D, McBoyle G (2007) Climate change adaptation in the ski industry. Mitig Adapt Strat Glob Change 12(8):1411–1431

Seidel K, Martinec J (2002) Hydrological applications of satellite snow cover mapping in the Swiss Alps. In: Proceedings of EARSeL-LISSIG-Workshop Observing our Cryosphere from Space, vol 80

Seidel K, Martinec J (2004) Remote sensing in snow hydrology: runoff modelling, effect of climate change. Springer-Praxis books in geophysical sciences. Springer, Praxis Pub., Berlin, New York, Chichester, UK, p 150

Steger C, Kotlarski S, Jonas T, Schär C (2013) Alpine snow cover in a changing climate: a regional climate model perspective. Clim Dyn 41(3–4):735–754. doi:10.1007/s00382-012-1545-3

Steiger R, Mayer M (2008) Snowmaking and climate change: future options for snow production in Tyrolean ski resorts. Mt Res Dev 28(3):292–298

Steppeler J, Doms G, Schättler U, Bitzer HW, Gassmann A, Damrath U, Gregoric G (2003) Meso-gamma scale forecasts using the nonhydrostatic model LM. Meteorol Atmos Phys 82(1–4):75–96. doi:10.1007/s00703-001-0592-9

Sun C, Walker JP, Houser PR (2004) A methodology for snow data assimilation in a land surface model. J Geophys Res Atmos 109(D8). doi:10.1029/2003JD003765

Takala M, Luojus K, Pulliainen J, Derksen C, Lemmetyinen J, Kärnä JP, Koskinen J, Bojkov B (2011) Estimating northern hemisphere snow water equivalent for climate research through assimilation of space-borne radiometer data and ground-based measurements. Remote Sens Environ 115(12):3517–3529. doi:10.1016/j.rse.2011.08.014

Taylor KE, Stouffer RJ, Meehl GA (2012) An overview of CMIP5 and the experiment design. Bull Am Meteorol Soc 93(4):485–498

Tedesco M, Narvekar P (2010) Assessment of the NASA AMSR-E SWE product. Selected topics in applied earth observations and remote sensing. IEEE J 3(1):141–159. doi:10.1109/JSTARS.2010.2040462

Tedesco M, Kelly R, Foster J, Chang A (2004) AMSR-E/Aqua daily l3 global snow water equivalent EASE-Grids V002. National Snow and Ice Data Center, Boulder

Theurillat JP, Guisan A (2001) Potential impact of climate change on vegetation in the European Alps: a review. Clim Change 50(1–2):77–109

Tiedtke M (1989) A comprehensive mass flux scheme for cumulus parameterization in large-scale models. Mon Weather Rev 117(8):1779–1800

Tong J, Déry SJ, Jackson PL (2009) Topographic control of snow distribution in an alpine watershed of western Canada inferred from spatially-filtered MODIS snow products. Hydrol Earth Syst Sci 13(3):319–326. doi:10.5194/hess-13-319-2009

Uppala SM, KÅllberg PW, Simmons AJ, Andrae U, Bechtold VDC, FiorinoM, Gibson JK, Haseler J, Hernandez A, Kelly GA, Li X, Onogi K,Saarinen S, Sokka N, Allan RP, Andersson E, Arpe K, Balmaseda MA,Beljaars ACM, Berg LVD, Bidlot J, Bormann N, Caires S, Chevallier F,Dethof A, Dragosavac M, Fisher M, Fuentes M, Hagemann S, Hólm E,Hoskins BJ, Isaksen L,

Janssen PAEM, Jenne R, Mcnally AP, MahfoufJF, Morcrette JJ, Rayner NA, Saunders RW, Simon P, Sterl A, Trenberth KE, Untch A, Vasiljevic D, Viterbo P, Woollen J (2005) The ERA-40 re-analysis. Q J R Meteorol Soc 131(612):2961–3012. doi:10.1256/qj.04.176

Vanham D (2012) The Alps under climate change: implications for water management in Europe. J Water Clim Change 3(3):197–206

Vavrus S (2007) The role of terrestrial snow cover in the climate system. Clim Dyn 29(1):73–88. doi:10.1007/s00382-007-0226-0

Viviroli D, Dürr HH, Messerli B, Meybeck M, Weingartner R (2007) Mountains of the world, water towers for humanity: typology, mapping, and global significance. Water Resour Res 43(7). doi:10.1029/2006WR005653

Voigt T, Füssel HM, Gärtner-Roer I, Huggel C, Marty C, Zemp M (2010) Impacts of climate change on snow, ice, and permafrost in Europe: observed trends, future projections, and socio-economic relevance. ETC/ACC Technical Paper 2010/13, The European Topic Centre on Air and Climate Change, Bilthovan, The Netherlands, p 117

Walther GR, Post E, Convey P, Menzel A, Parmesan C, Beebee TJ, Fromentin JM, Hoegh-Guldberg O, Bairlein F (2002) Ecological responses to recent climate change. Nature 416(6879):389–395

Weber RO, Talkner P, Auer I, Böhm R, Gajić-Čapka M, Zaninović K, Brazdil R, Faško P (1997) 20th-century changes of temperature in the mountain regions of central Europe. Clim Change 36(3–4):327–344

Wielke LM, Haimberger L, Hantel M (2004) Snow cover duration in Switzerland compared to Austria. Meteorol Z 13(1):13–17

Wilby RL, Wigley TML, Conway D, Jones PD, Hewitson BC, Main J, Wilks DS (1998) Statistical downscaling of general circulation model output: a comparison of methods. Water Resour Res 34(11):2995–3008. doi:10.1029/98WR02577

Wood A, Leung L, Sridhar V, Lettenmaier D (2004) Hydrologic implications of dynamical and statistical approaches to downscaling climate model outputs. Clim Change 62(1–3):189–216. doi:10.1023/B:CLIM.0000013685.99609.9e

Zaitchik BF, Rodell M (2009) Forward-looking assimilation of MODIS-derived snow-covered area into a land surface model. J Hydrometeorol 10(1):130–148